

## Silver(I) Complexes of *Bis-* and *Tris-(pyrazolyl)azine Derivatives – Dimers, Coordination Polymers and a Pentametallic Assembly*

Izar Capel Berdiell, Stuart L. Warriner and Malcolm A. Halcrow\*

*School of Chemistry, University of Leeds, Woodhouse Lane, Leeds LS2 9JT, UK.*  
*E-mail: m.a.halcrow@leeds.ac.uk.*

### Supporting Information

	Page
<b>Figure S1</b> $^1\text{H}$ and $^{13}\text{C}$ NMR spectra of bpt.	2
<b>Figure S2</b> View of the molecule in the crystal structure of bpt.	3
<b>Figure S3</b> Packing diagram of bpt.	3
<b>Figure S4</b> View of the dimeric cations in <b>1</b> ·2MeCN and <b>4</b> , showing the atom numbering schemes.	4
<b>Table S1</b> Selected bond lengths and angles for the crystal structures of <b>1</b> ·2MeCN and <b>3</b> .	5
<b>Figure S5</b> Comparison of the heterocyclic ligand dispositions in the dimeric cations in <b>1</b> ·2MeCN and <b>3</b> .	6
<b>Figure S6</b> Packing diagrams of <b>1</b> ·2MeCN and <b>3</b> , showing the canted stacks of dimeric cations.	7
<b>Table S2</b> Metric parameters for intramolecular and intermolecular $\pi\cdots\pi$ interactions in <b>1</b> ·2MeCN and <b>3</b> .	8
<b>Figure S7</b> View of the asymmetric unit in $\alpha$ - <b>2</b> ·½MeNO <sub>2</sub> .	8
<b>Figure S8</b> View of the asymmetric unit in $\beta$ - <b>2</b> ·xMeNO <sub>2</sub> .	9
<b>Table S3</b> Selected bond lengths and angles for $\alpha$ - <b>2</b> ·½MeNO <sub>2</sub> and $\beta$ - <b>2</b> ·xMeNO <sub>2</sub> .	10
<b>Table S4</b> Metric parameters for intra-dimer $\pi\cdots\pi$ interactions in $\alpha$ - <b>2</b> ·MeNO <sub>2</sub>	11
<b>Figure S9</b> Packing diagram of $\alpha$ - <b>2</b> ·MeNO <sub>2</sub> , showing the well-separated coordination polymer chains.	11
<b>Figure S10</b> An extended helical chain in $\beta$ - <b>2</b> ·yMeNO <sub>2</sub> , plotted with displacement ellipsoids and space-filling views.	12
<b>Table S5</b> Metric parameters for intramolecular $\pi\cdots\pi$ contacts in $\beta$ - <b>2</b> ·yMeNO <sub>2</sub> .	13
<b>Figure S11</b> Packing diagram of $\beta$ - <b>2</b> ·yMeNO <sub>2</sub> , showing the alternating stripes of $\Lambda$ and $\Delta$ helical chains.	13
<b>Figure S12</b> View of the pentanuclear $[\text{Ag}_5(\text{tpym})_4(\text{BF}_4)_2]^{3+}$ assembly in <b>4</b> ·2MeNO <sub>2</sub> .	14
<b>Table S6</b> Selected bond lengths and angles for <b>4</b> ·2MeNO <sub>2</sub> .	14
<b>Table S7</b> Metric parameters for intramolecular and intermolecular $\pi\cdots\pi$ interactions in <b>4</b> ·2MeNO <sub>2</sub> .	15
<b>Figure S13</b> Packing diagram of <b>4</b> ·2MeNO <sub>2</sub> , showing the anion- and solvent-filled voids in the lattice.	15
<b>Figure S14</b> Space-filling packing diagram of <b>4</b> ·2MeNO <sub>2</sub> , showing the anion- and solvent-filled voids.	16
<b>Figure S15</b> Views of the asymmetric units of isostructural <b>5a</b> and <b>5b</b> .	17
<b>Table S8</b> Selected bond lengths and angles for isostructural <b>5a</b> and <b>5b</b> .	18
<b>Figure S16</b> Packing diagrams of <b>5a</b> , showing the coparallel helical chains in the lattice.	19
<b>Figure S17</b> Views of the coordination polymer asymmetric unit of <b>5a</b> ·MeNO <sub>2</sub> .	20
<b>Table S9</b> Selected bond lengths and angles for <b>5a</b> ·MeNO <sub>2</sub> .	21
<b>Table S10</b> Metric parameters for intra-chain and inter-chain $\pi\cdots\pi$ interactions in <b>5a</b> ·MeNO <sub>2</sub>	21
<b>Figure S18</b> Packing diagram of <b>5a</b> ·MeNO <sub>2</sub> , showing the anion... $\pi$ interactions linking the coordination polymer chains.	22
<b>Figure S19</b> Packing diagram of <b>5a</b> ·MeNO <sub>2</sub> , showing the coordination polymer/anion... $\pi$ layers separated by anions and solvent.	22
<b>Figure S20</b> View of the full asymmetric unit of <b>5a</b> ·MeOH.	23
<b>Table S11</b> Selected bond lengths and angles for <b>5a</b> ·MeOH.	23
<b>Table S12</b> Hydrogen bond parameters for <b>5a</b> ·MeOH.	24
<b>Figure S21</b> Packing diagram of <b>5a</b> ·MeOH, showing well-separated polymer chains.	24
<b>Figure S22</b> View of the $\{[\text{Ag}(\text{bpt})]\text{BF}_4\}_n$ coordination polymer chain in <b>6</b> .	25
<b>Table S13</b> Selected bond lengths and angles for <b>6</b> .	25
<b>Figure S23</b> Packing diagrams of <b>6</b> , showing the coordination polymer chains and anion... $\pi$ . interactions.	26
<b>Figure S24</b> X-ray powder diffraction data from the tpp and tpym complexes <b>1</b> - <b>4</b> .	27
<b>Figure S25</b> X-ray powder diffraction data from the tpt and bpt complexes <b>5a</b> / <b>5b</b> and <b>6</b> .	28
<b>Figure S26</b> Electrospray mass spectra of the complexes from MeNO <sub>2</sub> solution.	29

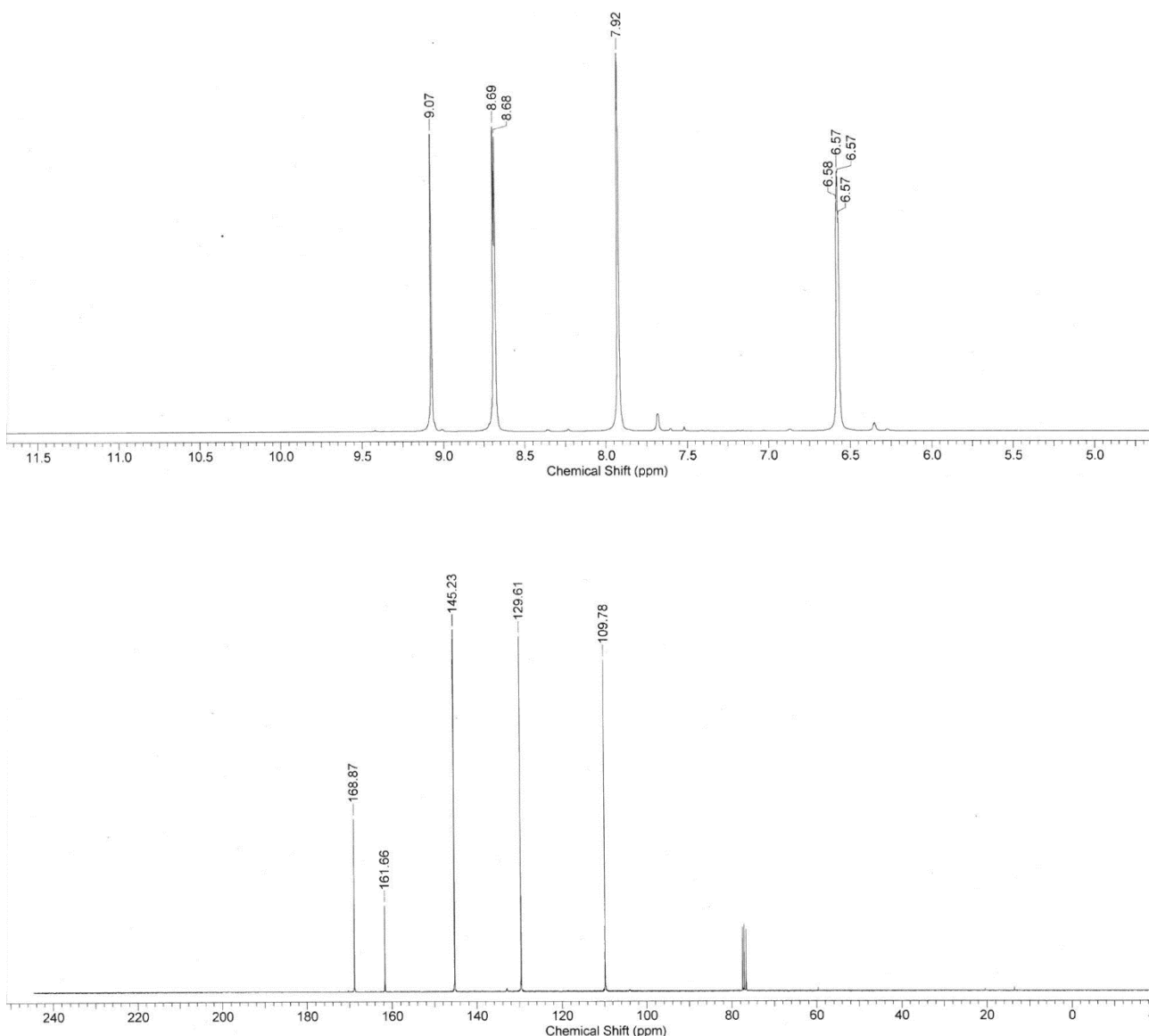


**Figure S1.**  $^1\text{H}$  (top) and  $^{13}\text{C}$  (bottom) NMR spectra of the new ligand bpt in  $\text{CDCl}_3$ .

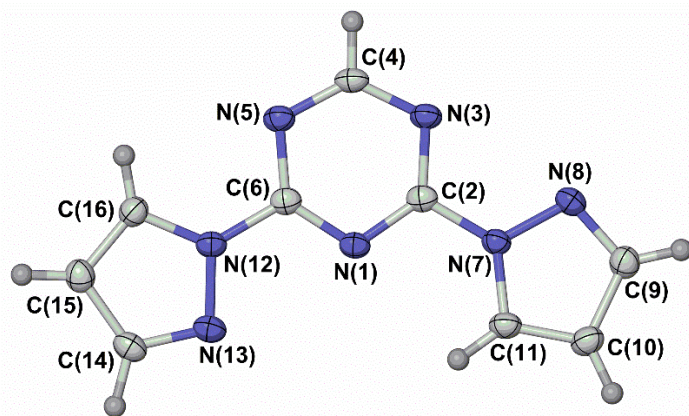


**Figure S2.** View of the molecule in the crystal structure of bpt, showing the atom numbering scheme. Atomic displacement ellipsoids are at the 50 % probability level, except for H atoms which have arbitrary radii.

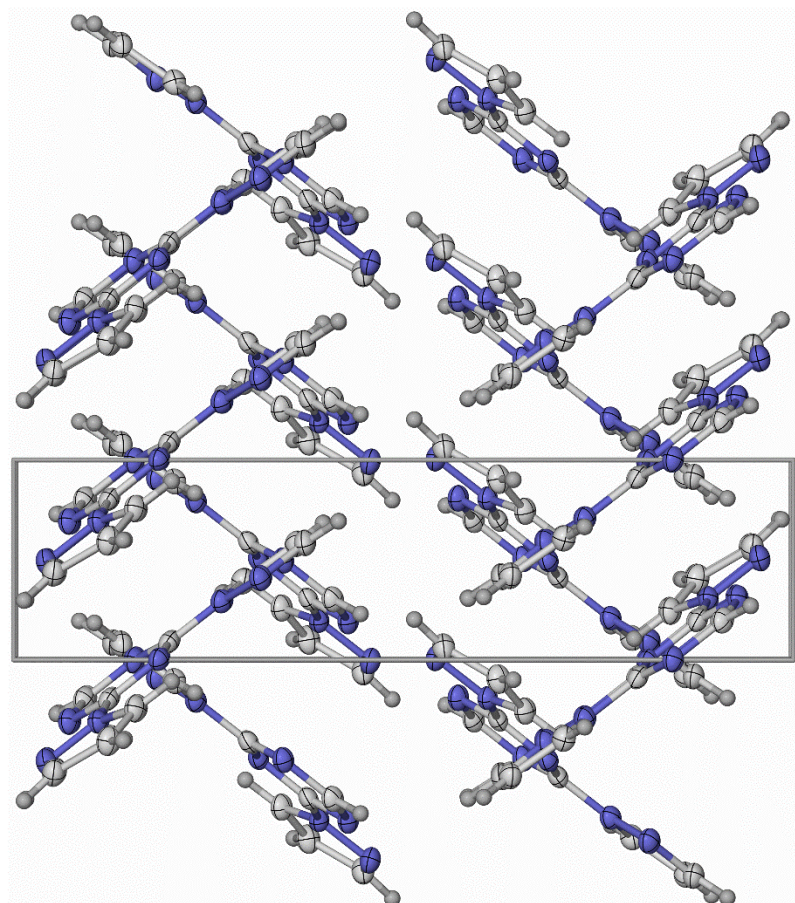


**Figure S3.** Packing diagram of bpt, showing the organisation of the molecules into canted stacks by translation along the unit cell *b* direction. The view is parallel to the [100] crystal vector, with *b* vertical. The interplanar distance between the stacked molecules is 3.267(2) Å.

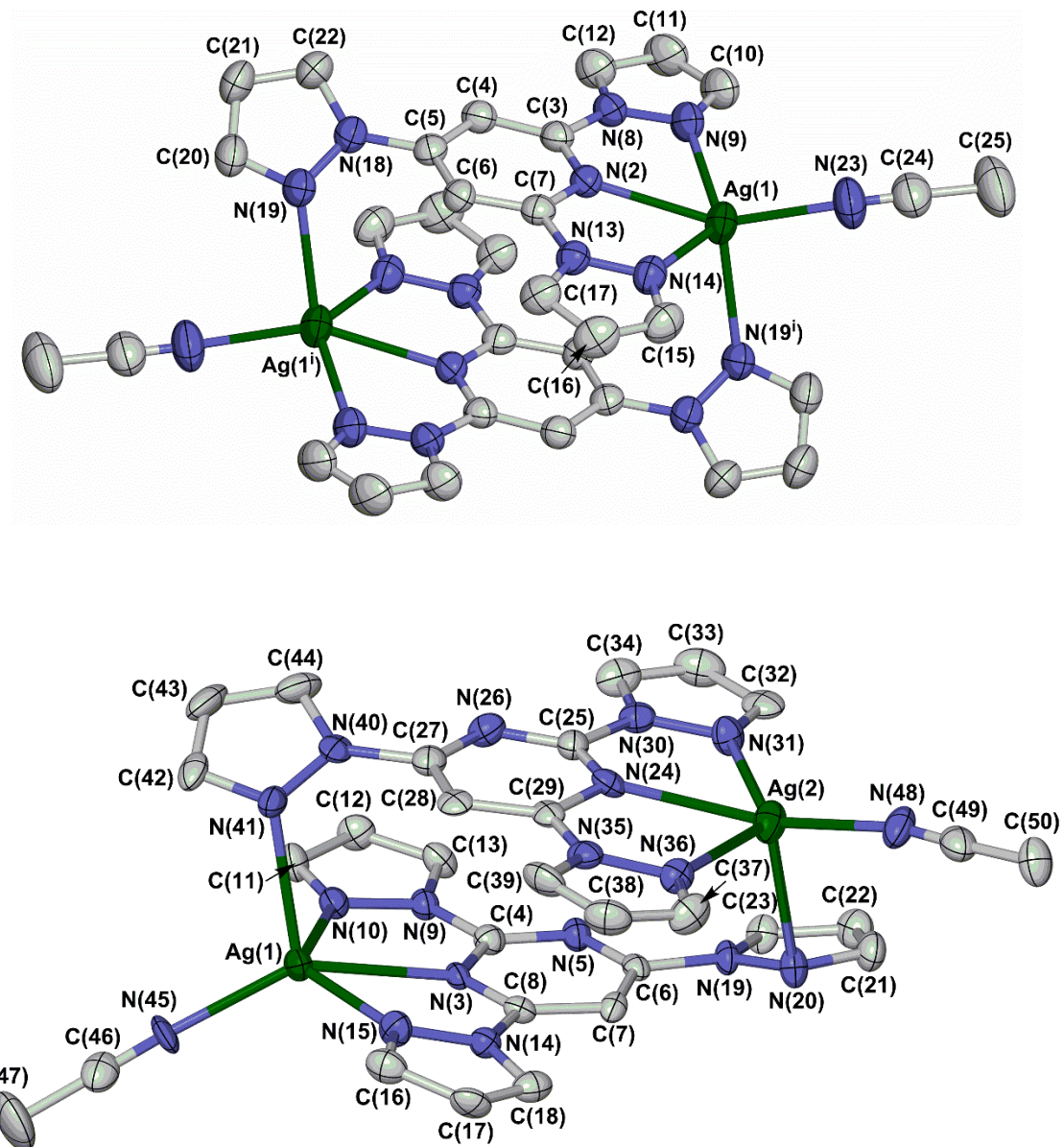


**Figure S4.** View of the  $[\text{Ag}_2(\text{tpp})_2(\text{NCMe})_2]^{2+}$  cation in **1**·2MeCN (top) and of  $[\text{Ag}_2(\text{tpym})_2(\text{NCMe})_2]^{2+}$  in **3** (bottom), showing the full atom numbering schemes. Atomic displacement ellipsoids are at the 50 % probability level, and H atoms are omitted for clarity. Symmetry code: (i)  $1-x, 1-y, 1-z$ .

Colour code: C, white; Ag, green; N, blue.

**Table S1.** Selected bond lengths ( $\text{\AA}$ ) and angles ( $^\circ$ ) for the crystal structures of the dimeric acetonitrile solvates  $[\text{Ag}_2(\text{tpy})_2(\text{NCMe})_2][\text{BF}_4]_2 \cdot 2\text{MeCN}$  (**1**·2MeCN) and  $[\text{Ag}_2(\text{tpym})_2(\text{NCMe})_2][\text{BF}_4]_2$  (**3**), including intramolecular Ag...Ag distances. See Fig. S4 for the atom numbering schemes employed. Symmetry code: (i)  $1-x, 1-y, 1-z$ .

<b>1</b> ·2MeCN		<b>3</b>	
Ag(1)–N(2)	2.445(3)	Ag(1)–N(3)	2.449(7)
Ag(1)–N(9)	2.461(5)	Ag(1)–N(10)	2.557(8)
Ag(1)–N(14)	2.414(4)	Ag(1)–N(15)	2.384(8)
Ag(1)–N(19 <sup>i</sup> )	2.566(4)	Ag(1)–N(41)	2.497(8)
Ag(1)–N(23)	2.250(5)	Ag(1)–N(45)	2.207(8)
		Ag(2)–N(20)	2.621(9)
		Ag(2)–N(24)	2.428(8)
		Ag(2)–N(31)	2.400(7)
		Ag(2)–N(36)	2.531(7)
		Ag(2)–N(48)	2.194(9)
N(2)–Ag(1)–N(9)	65.74(12)	N(3)–Ag(1)–N(10)	64.6(2)
N(2)–Ag(1)–N(14)	65.92(12)	N(3)–Ag(1)–N(15)	66.1(2)
N(2)–Ag(1)–N(19 <sup>i</sup> )	113.38(12)	N(3)–Ag(1)–N(41)	106.3(2)
N(2)–Ag(1)–N(23)	153.60(18)	N(3)–Ag(1)–N(45)	143.5(3)
N(9)–Ag(1)–N(14)	131.02(13)	N(10)–Ag(1)–N(15)	130.7(2)
N(9)–Ag(1)–N(19 <sup>i</sup> )	117.25(14)	N(10)–Ag(1)–N(41)	85.6(3)
N(9)–Ag(1)–N(23)	99.44(19)	N(10)–Ag(1)–N(45)	107.9(3)
N(14)–Ag(1)–N(19 <sup>i</sup> )	88.88(13)	N(15)–Ag(1)–N(41)	106.9(3)
N(14)–Ag(1)–N(23)	121.21(19)	N(15)–Ag(1)–N(45)	112.2(3)
N(19 <sup>i</sup> )–Ag(1)–N(23)	92.70(18)	N(41)–Ag(1)–N(45)	108.7(3)
		N(20)–Ag(2)–N(24)	108.2(2)
		N(20)–Ag(2)–N(31)	90.3(3)
		N(20)–Ag(2)–N(36)	105.1(3)
		N(20)–Ag(2)–N(48)	97.8(3)
		N(24)–Ag(2)–N(31)	67.3(3)
		N(24)–Ag(2)–N(36)	64.2(2)
		N(24)–Ag(2)–N(48)	149.1(3)
		N(31)–Ag(2)–N(36)	131.5(3)
		N(31)–Ag(2)–N(48)	130.3(3)
		N(36)–Ag(2)–N(48)	93.5(3)
Ag(1)...Ag(1 <sup>i</sup> )	7.2461(7)	Ag(1)...Ag(2)	7.2706(10)
$\tau[\text{Ag}(1)]^a$	0.38	$\tau[\text{Ag}(1)]^a$	0.21
		$\tau[\text{Ag}(2)]^a$	0.29

<sup>a</sup>See ref. [1] for the definition of  $\tau$ . An ideal square pyramidal geometry gives  $\tau = 0$ , while an ideal trigonal bipyramidal geometry yields  $\tau = 1$ .

- [1] A. W. Addison, T. N. Rao, J. Reedijk, J. van Rijn and G. C. Verschoor, *J. Chem. Soc., Dalton Trans.*, 1984, 1349.

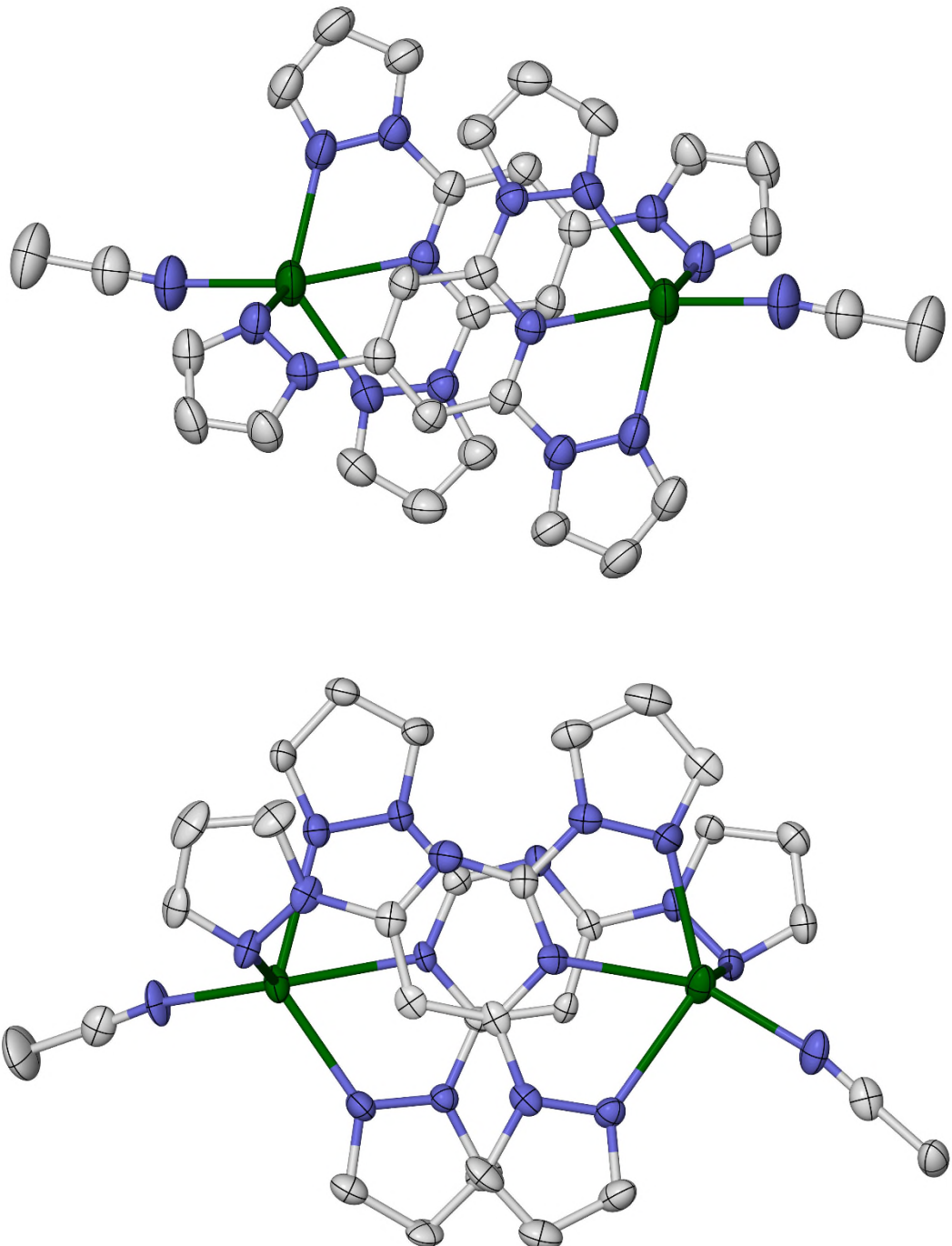


**Figure S5.** Comparison of centrosymmetric  $[\text{Ag}_2(\text{tpp})_2(\text{NCMe})_2]^{2+}$  in **1**·2MeCN (top) and  $C_1$ -symmetric  $[\text{Ag}_2(\text{tpym})_2(\text{NCMe})_2]^{2+}$  in **3** (bottom). The views are perpendicular to the least squares planes of the tridentate ligand domains. Other details as for Figure S4. Colour code: C, white; Ag, green; N, blue.

The compounds differ in the relative dispositions of the monodentate pyrazolyl groups on each ligand, which are *transoid* to each other in **1**·2MeCN and *cisoid* in **3**.

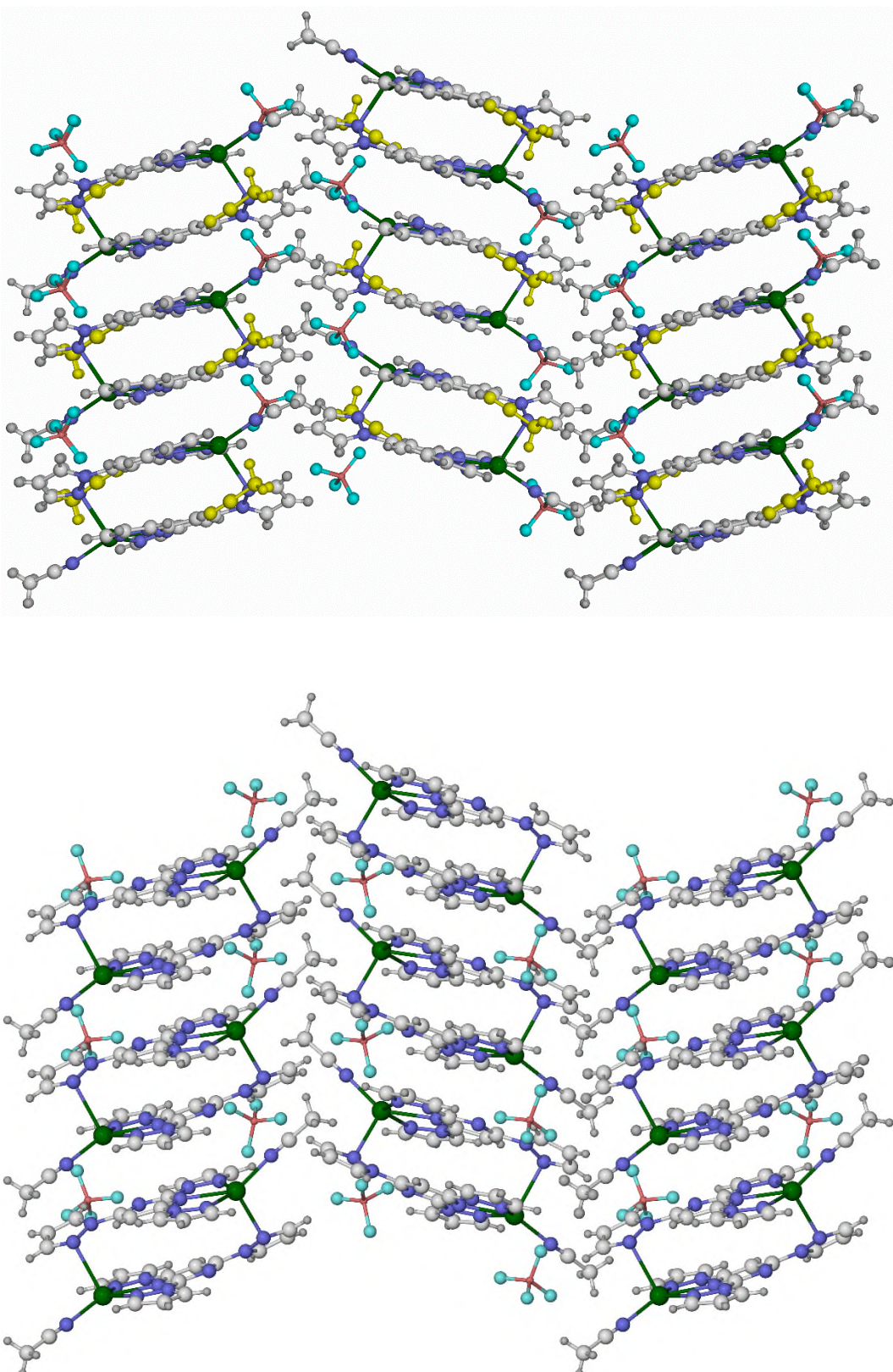


**Figure S6.** Packing diagrams of **1·2MeCN** (top) and **3** (bottom), showing the canted stacks of dimeric cations parallel to the unit cell *b* direction. The views are both along the [100] crystal vector, with *b* vertical. Only one orientation of the disordered residues is shown, and all atoms have arbitrary radii. Colour code: C, white; H, pale grey; Ag, green; B, pink; F, cyan; N, blue; lattice MeCN, yellow.

**Table S2.** Metric parameters for  $\pi\ldots\pi$  interactions in **1·2MeCN** and **3** ( $\text{\AA}$ ,  $^\circ$ ). See Fig. S4 for the atom numbering scheme employed. Symmetry codes: (i)  $1-x$ ,  $1-y$ ,  $1-z$ ; (ii)  $1-x$ ,  $-y$ ,  $1-z$ ; (iii)  $x$ ,  $1+y$ ,  $z$ .

	Dihedral angle	Interplanar distance	Horizontal offset
<b>1·2MeCN</b>			
Intramolecular [N(2)–C(7)]...[N(2 <sup>i</sup> )...C(7 <sup>i</sup> )]	0	3.338(3)	1.92
Intermolecular [N(2)–C(7)]...[N(13 <sup>ii</sup> )...C(17 <sup>ii</sup> )]	4.35(14)	3.395(17)	1.89
<b>3</b>			
Intramolecular [N(3)–C(8)]...[N(24)...C(29)]	1.7(3)	3.28(3)	0.59
Intermolecular [N(3)–C(8)]...[N(24 <sup>iii</sup> )...C(24 <sup>iii</sup> )]	1.7(3)	3.19(3)	2.92

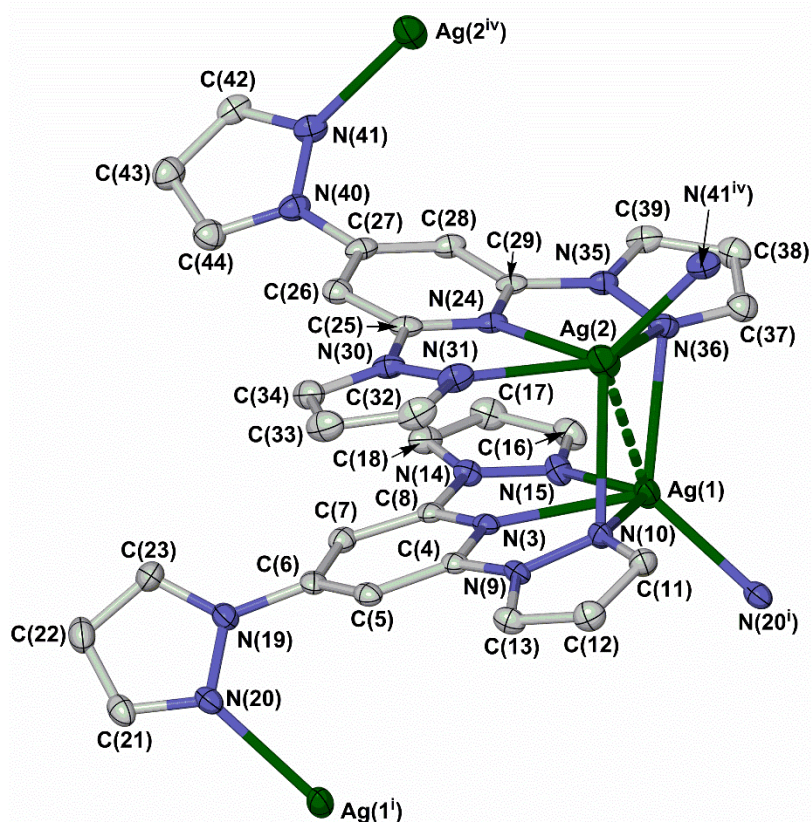


**Figure S7.** View of the  $[\text{Ag}_2(\text{tpp})_2]^{2+}$  moiety in the asymmetric unit of  $\alpha\text{-}2\cdot\text{MeNO}_2$ , showing the full atom numbering scheme. Details as for Figure S4. Symmetry codes: (i)  $1-x$ ,  $1-y$ ,  $1-z$ ; (iv)  $1-x$ ,  $1-y$ ,  $-z$ .

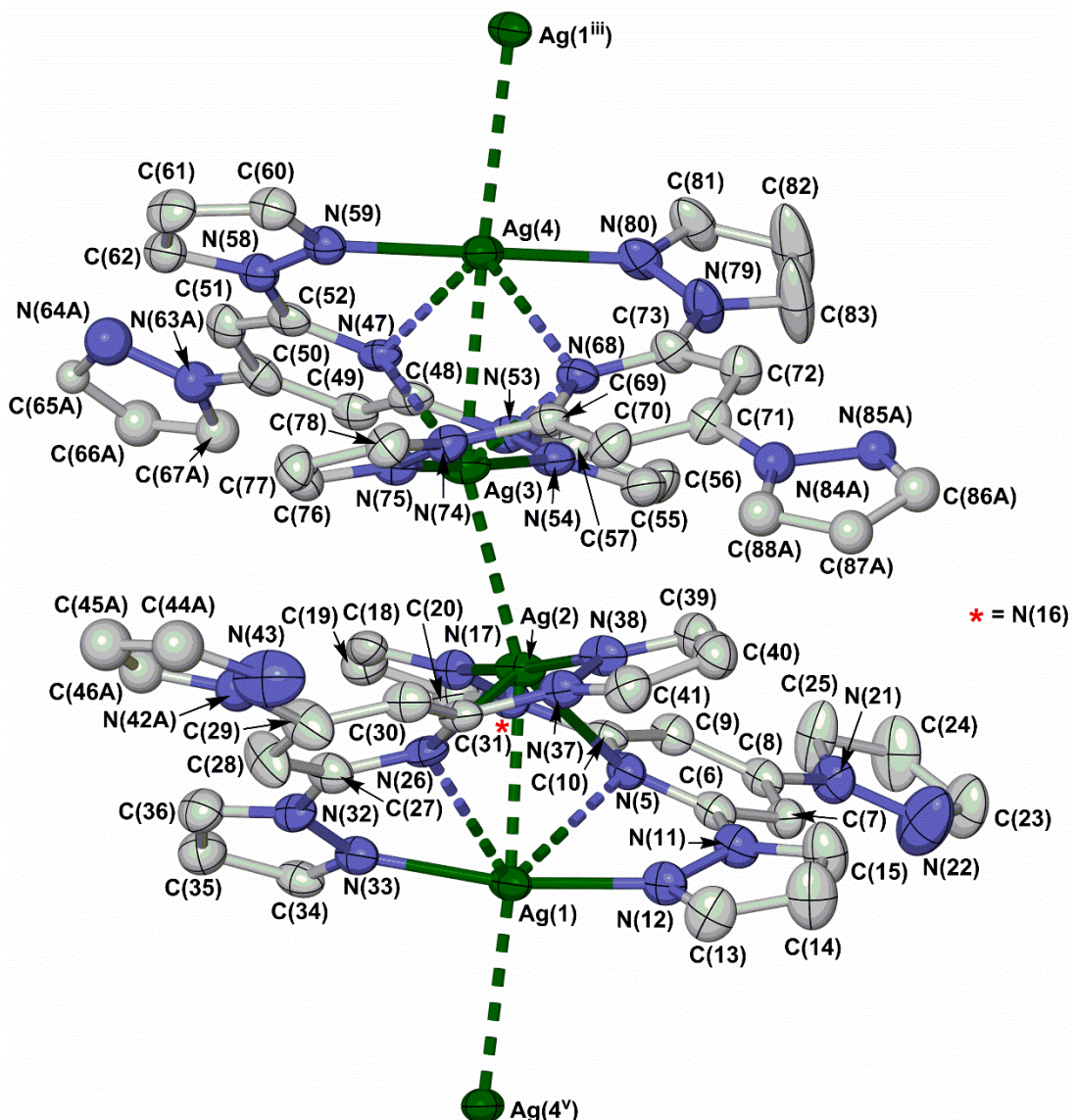


**Figure S8.** View of the unique  $\{[\text{Ag}_2(\text{tpp})_2]_2\}^{4+}$  moiety in the asymmetric unit of  $\beta\text{-2}\cdot y\text{MeNO}_2$ , showing the full atom numbering scheme. Details as for Figure S4. Symmetry codes: (iii)  $x, 1+y, z$ ; (v)  $x, -1+y, z$ .

**Table S3.** Selected bond lengths ( $\text{\AA}$ ) and angles ( $^\circ$ ) for the solvatomorphs  $[\text{Ag}_2(\text{tpp})_2][\text{BF}_4]_2 \cdot \text{MeNO}_2$  ( $\alpha\text{-2}\cdot\text{MeNO}_2$ ) and  $[\text{Ag}_2(\text{tpp})_2][\text{BF}_4]_2 \cdot y\text{MeNO}_2$  ( $\beta\text{-2}\cdot y\text{MeNO}_2$ ), including intramolecular  $\text{Ag} \dots \text{Ag}$  distances. See Figs. S7 and S8 for the atom numbering schemes employed. Symmetry codes: (i)  $1-x, 1-y, 1-z$ ; (iv)  $1-x, 1-y, -z$ ; (v)  $x, -1+y, z$ .

$\alpha\text{-2}\cdot\text{MeNO}_2$	$\beta\text{-2}\cdot y\text{MeNO}_2$
Ag(1)–N(3)	2.487(2)
Ag(1)–N(10)	2.590(2)
Ag(1)–N(15)	2.389(2)
Ag(1)–N(20 <sup>i</sup> )	2.272(2)
Ag(1)–N(36)	2.520(2)
Ag(2)–N(10)	2.610(2)
Ag(2)–N(24)	2.484(2)
Ag(2)–N(31)	2.356(2)
Ag(2)–N(36)	2.636(2)
Ag(2)–N(41 <sup>iv</sup> )	2.292(2)
N(3)–Ag(1)–N(9)	63.39(7)
N(3)–Ag(1)–N(15)	67.08(7)
N(3)–Ag(1)–N(20 <sup>i</sup> )	126.47(7)
N(3)–Ag(1)–N(36)	106.23(7)
N(10)–Ag(1)–N(15)	130.36(7)
N(10)–Ag(1)–N(20 <sup>i</sup> )	94.94(8)
N(10)–Ag(1)–N(36)	103.95(7)
N(15)–Ag(1)–N(20 <sup>i</sup> )	117.44(8)
N(15)–Ag(1)–N(36)	86.31(8)
N(20 <sup>i</sup> )–Ag(1)–N(36)	126.92(8)
N(10)–Ag(2)–N(24)	101.71(7)
N(10)–Ag(2)–N(31)	83.61(7)
N(10)–Ag(2)–N(36)	103.95(7)
N(10)–Ag(2)–N(41 <sup>iv</sup> )	131.09(8)
N(24)–Ag(2)–N(31)	67.32(8)
N(24)–Ag(2)–N(36)	62.93(7)
N(24)–Ag(2)–N(41 <sup>iv</sup> )	125.51(7)
N(31)–Ag(2)–N(36)	129.86(8)
N(31)–Ag(2)–N(41 <sup>iv</sup> )	123.23(8)
N(36)–Ag(2)–N(41 <sup>iv</sup> )	91.57(7)
Ag(1)...Ag(2)	3.2497(4)
Ag(1)...Ag(1 <sup>i</sup> )	6.8167(7)
Ag(2)...Ag(2 <sup>iv</sup> )	6.8762(7)
$\tau[\text{Ag}(1)]^a$	0.06
$\tau[\text{Ag}(2)]^a$	0.02
Ag(1)–N(5)	2.845(5)
Ag(1)–N(12)	2.154(6)
Ag(1)–N(26)	2.759(5)
Ag(1)–N(33)	2.153(5)
Ag(2)–N(5)	2.605(5)
Ag(2)–N(17)	2.175(5)
Ag(2)–N(26)	2.547(5)
Ag(2)–N(38)	2.200(5)
Ag(3)–N(47)	2.658(5)
Ag(3)–N(54)	2.176(5)
Ag(3)–N(68)	2.712(5)
Ag(3)–N(75)	2.147(5)
Ag(4)–N(47)	2.755(5)
Ag(4)–N(59)	2.159(5)
Ag(4)–N(68)	2.787(5)
Ag(4)–N(80)	2.162(5)
N(5)–Ag(1)–N(12)	66.16(17)
N(5)–Ag(1)–N(26)	106.82(14)
N(5)–Ag(1)–N(33)	109.47(17)
N(12)–Ag(1)–N(26)	105.42(17)
N(12)–Ag(1)–N(33)	169.90(19)
N(26)–Ag(1)–N(33)	66.48(17)
N(5)–Ag(2)–N(17)	68.89(17)
N(5)–Ag(2)–N(26)	121.70(15)
N(5)–Ag(2)–N(38)	107.88(17)
N(17)–Ag(2)–N(26)	118.45(17)
N(17)–Ag(2)–N(38)	171.60(18)
N(26)–Ag(2)–N(38)	69.93(17)
N(47)–Ag(3)–N(54)	68.55(17)
N(47)–Ag(3)–N(68)	118.29(14)
N(47)–Ag(3)–N(75)	115.86(17)
N(54)–Ag(3)–N(68)	103.77(17)
N(54)–Ag(3)–N(75)	171.97(19)
N(68)–Ag(3)–N(75)	68.31(17)
N(47)–Ag(4)–N(59)	66.11(17)
N(47)–Ag(4)–N(68)	112.59(14)
N(47)–Ag(4)–N(80)	112.82(17)
N(59)–Ag(4)–N(68)	114.70(17)
N(59)–Ag(4)–N(80)	178.51(18)
N(68)–Ag(4)–N(80)	66.59(16)
Ag(1)...Ag(2)	2.9089(6)
Ag(1)...Ag(4 <sup>v</sup> )	3.0660(6)
Ag(2)...Ag(3)	3.0415(6)
Ag(3)...Ag(4)	2.9108(6)

<sup>a</sup>See ref. [1] for the definition of  $\tau$  (page 4). An ideal square pyramidal geometry gives  $\tau = 0$ , while an ideal trigonal bipyramidal geometry yields  $\tau = 1$ .

**Table S4.** Metric parameters for intra-dimer  $\pi \dots \pi$  interactions in  $\alpha\text{-2-MeNO}_2$  ( $\text{\AA}$ ,  $^\circ$ ). See Fig. S7 for the atom numbering scheme employed. Symmetry codes: (i)  $1-x, 1-y, 1-z$ ; (ii)  $1-x, 1-y, -z$ ; (v)  $1-x, -y, 1-z$ .

	Dihedral angle	Interplanar distance	Horizontal offset
[N(3)–C(8)]...[N(3 <sup>i</sup> )...C(8 <sup>i</sup> )]	0	3.255(6)	2.00
[N(24)–C(29)]...[N(24 <sup>ii</sup> )...C(29 <sup>ii</sup> )]	0	3.221(9)	2.11

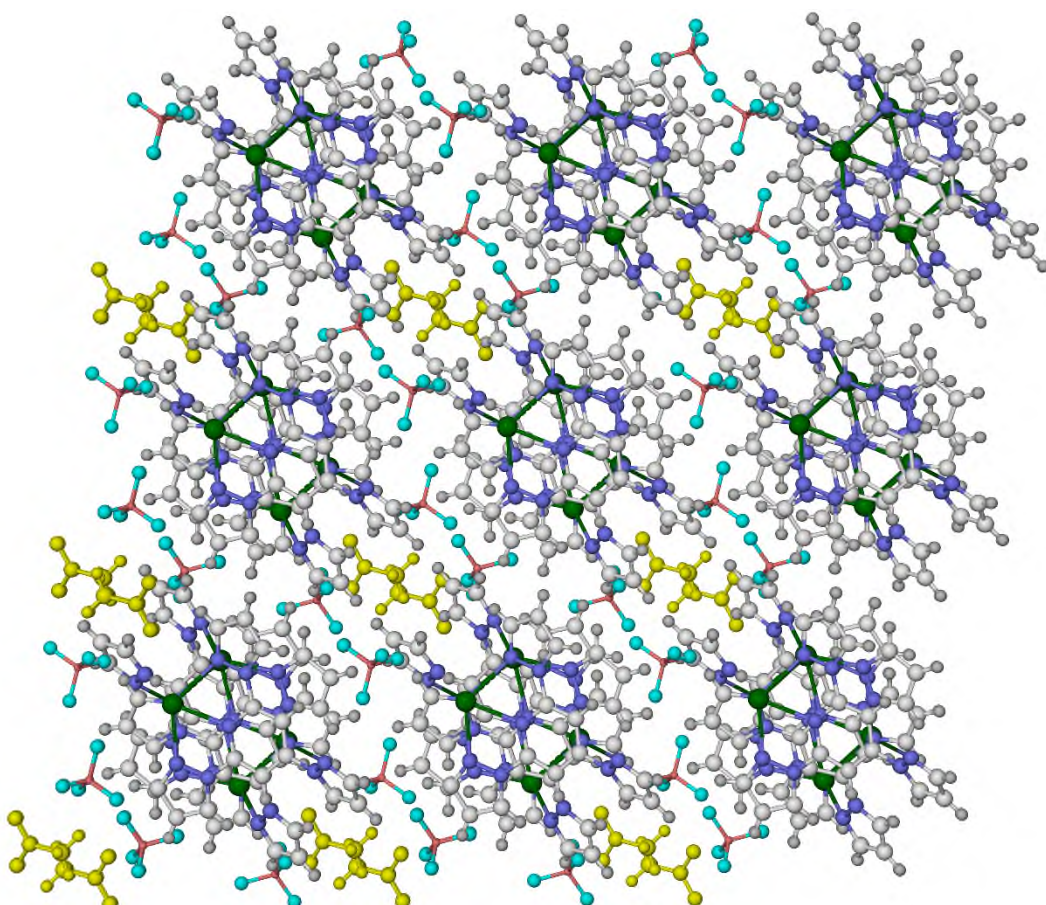


**Figure S9.** Packing diagram of  $\alpha\text{-2-MeNO}_2$ , showing the well-separated coordination polymer chains in the lattice. The view is along the [001] crystal vector, with the  $b$  axis horizontal. Only one orientation of the disordered solvent molecule is shown, and all atoms have arbitrary radii. Colour code: C, white; H, pale grey; Ag, green; B, pink; F, cyan; N, blue; MeNO<sub>2</sub>, yellow.

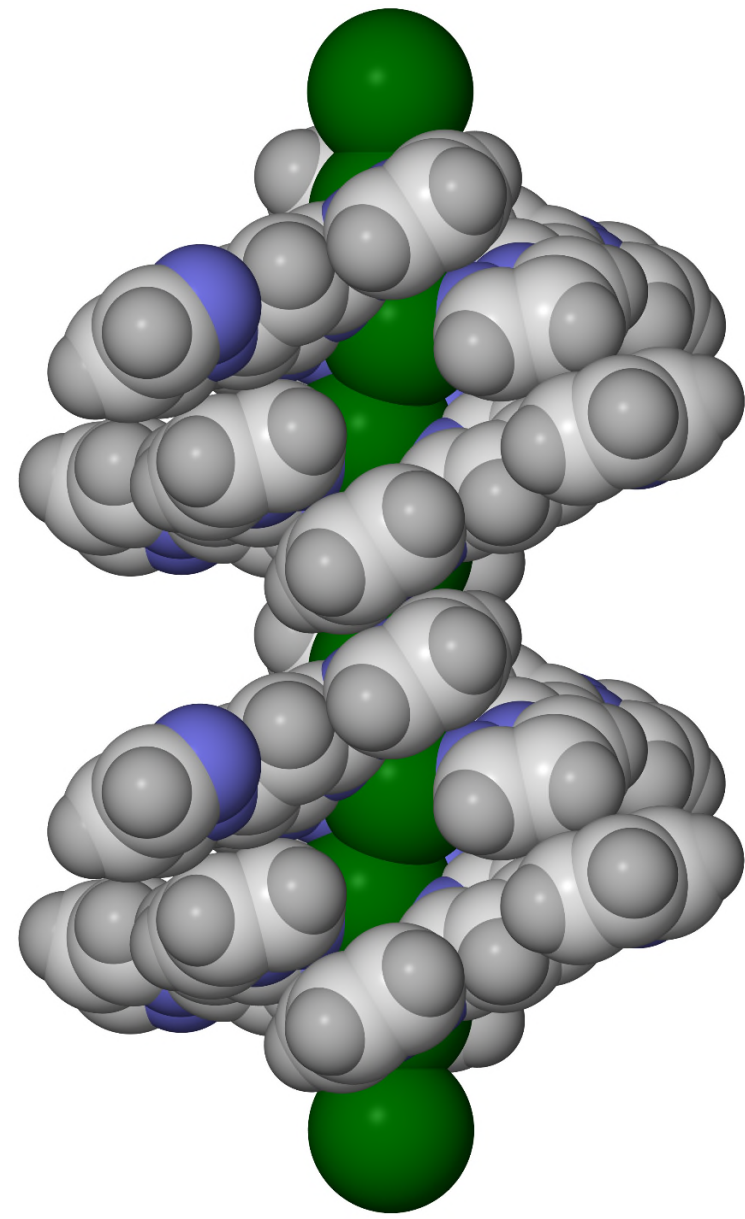
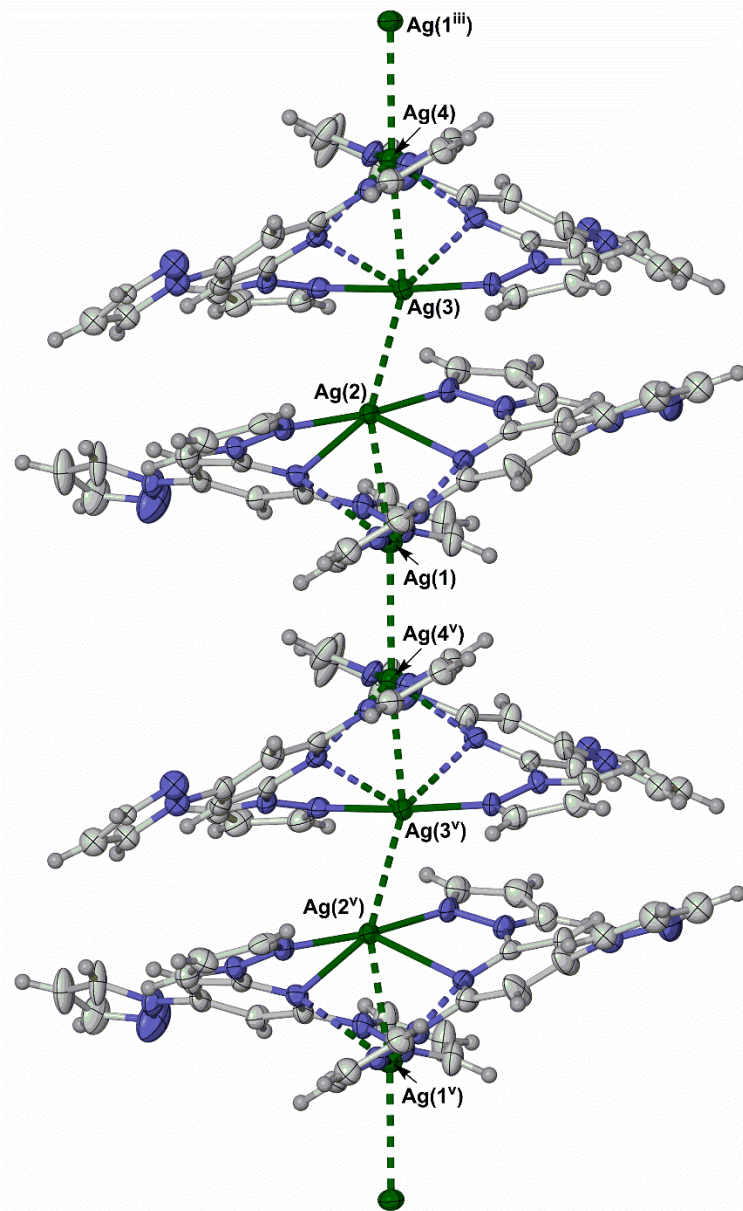


**Figure S10.** An extended helical chain in  $\beta$ -2-yMeNO<sub>2</sub>, plotted with 50 % displacement ellipsoids (left) and space-filling view (right). Only one orientation of the disordered pyrazolyl groups is shown; other details as for Figure S4. Symmetry codes: (iii)  $x, 1+y, z$ ; (v)  $x, -1+y, z$ .

**Table S5.** Metric parameters for intramolecular  $\pi \dots \pi$  contacts in  $\beta\text{-2}\cdot\gamma\text{MeNO}_2$  ( $\text{\AA}$ ,  $^\circ$ ). See Fig. S8 for the atom numbering scheme employed.

	Dihedral angle	Interplanar distance	Horizontal offset
[N(11)–C(15)]...[N(37)...C(41)]	12.7(3)	3.60(2)	1.45
[N(16)–C(20)]...[N(32)...C(36)]	16.6(3)	3.54(2)	2.23
[N(16)–C(20)]...[N(53)...C(57)]	14.7(3)	3.20(2)	2.07
[N(26)–C(31)]...[N(74)...C(78)]	9.9(3)	3.54(2)	1.65
[N(37)–C(41)]...[N(68)...C(73)]	12.3(3)	3.62(2)	1.04

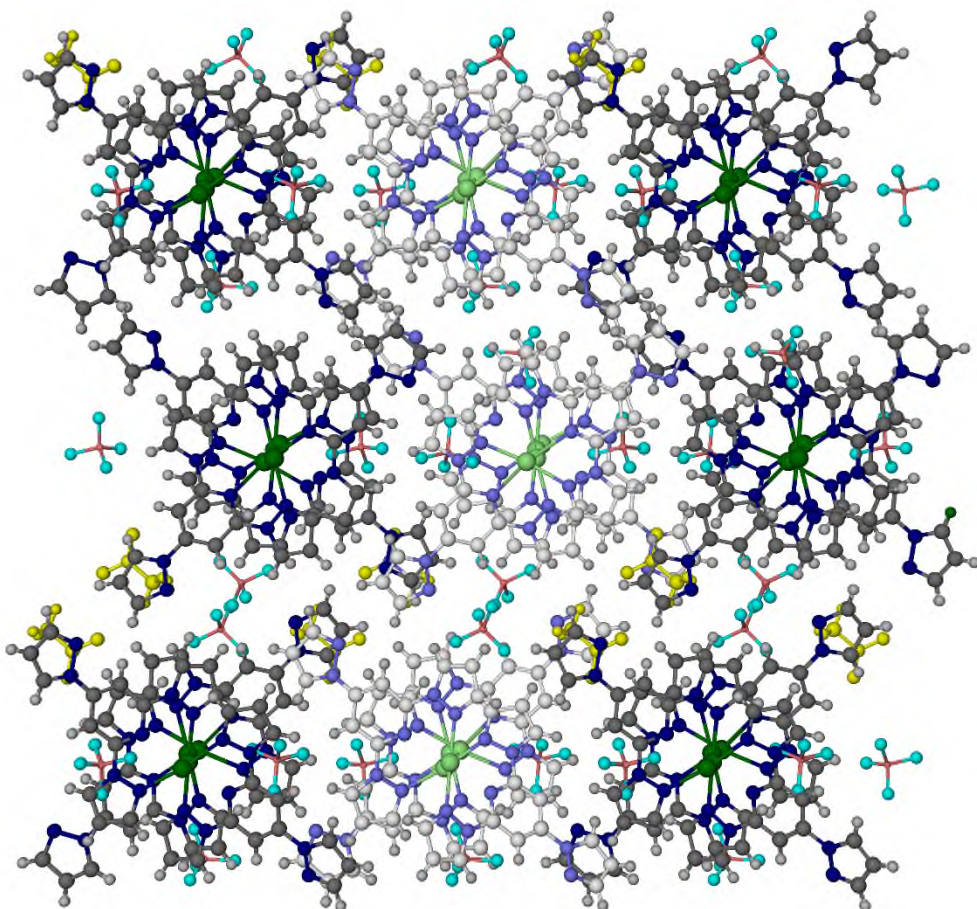


**Figure S11.** Packing diagram of  $\beta\text{-2}\cdot\gamma\text{MeNO}_2$ , showing the alternating stripes of  $\Lambda$  (dark colouration) and  $\Delta$  (pale colouration) helical chains in the lattice. The view shows the (010) crystal plane, with the  $c$  axis horizontal. Only one orientation of the disordered pyrazolyl groups is shown, and all atoms have arbitrary radii. Colour code: C, dark grey or white; H, pale grey; Ag, dark or pale green; B, pink; F, cyan; N, dark or pale blue;  $\text{MeNO}_2$ , yellow.

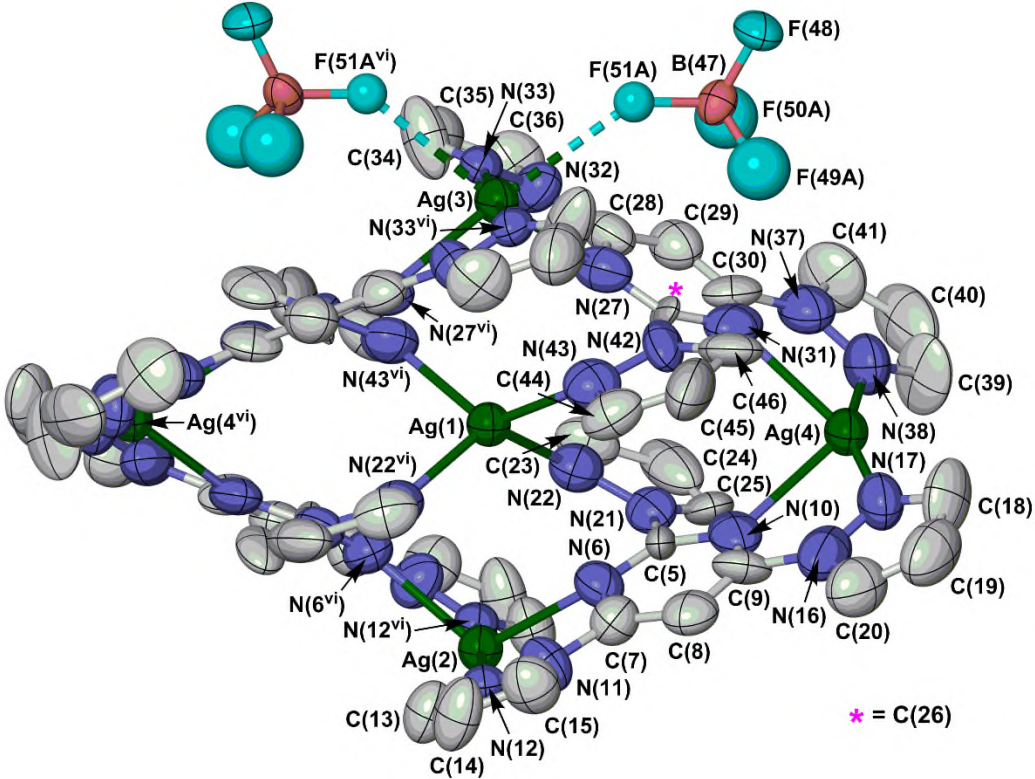


**Figure S12.** View of the pentanuclear  $[\text{Ag}_5(\text{tpym})_4(\text{BF}_4)_2]^{3+}$  assembly in **4**·2MeNO<sub>2</sub>, showing the full atom numbering scheme. Only one orientation of the disordered  $\text{BF}_4^-$  ion is shown. Other details as for Figure S4. Symmetry code: (vi)  $1-x, y, \frac{3}{2}-z$ . Colour code: C, white; Ag, green; B, pink; F, cyan; N, blue.

**Table S6.** Selected bond lengths ( $\text{\AA}$ ) and angles ( $^\circ$ ) for **4**·2MeNO<sub>2</sub>, including intramolecular Ag...Ag distances. See Fig. S12 for the atom numbering scheme employed. Symmetry code: (vi)  $1-x, y, \frac{3}{2}-z$ .

Ag(1)–N(22)	2.374(11)	Ag(3)–N(33)	2.240(10)
Ag(1)–N(43)	2.366(10)	Ag(3)–F(51A/B/C)	2.771(13)/2.902(17)/2.98(2)
Ag(2)–N(6)	2.491(10)	Ag(4)–N(10)	2.578(11)
Ag(2)–N(12)	2.238(10)	Ag(4)–N(17)	2.282(13)
Ag(3)–N(27)	2.498(10)	Ag(4)–N(31)	2.563(11)
		Ag(4)–N(38)	2.216(14)
N(22)–Ag(1)–N(22 <sup>xviii</sup> )	128.6(5)	N(27)–Ag(3)–F(51A/B/C <sup>xviii</sup> )	76.7(4)/70.7(4)/79.6(4)
N(22)–Ag(1)–N(43)	97.7(3)	N(33)–Ag(3)–N(33 <sup>xviii</sup> )	176.1(4)
N(22)–Ag(1)–N(43 <sup>xviii</sup> )	104.2(4)	N(33)–Ag(3)–F(51A/B/C)	84.4(6)/97.3(5)/73.8(5)
N(43)–Ag(1)–N(43 <sup>xviii</sup> )	128.1(5)	N(33)–Ag(3)–F(51A/B/C <sup>xviii</sup> )	93.1(6)/80.4(5)/103.9(5)
N(6)–Ag(2)–N(6 <sup>xviii</sup> )	114.4(5)	F(51A/B/C)–Ag(3)–F(51A/B/C <sup>xviii</sup> )	103.2(5)–109.6(7)
N(6)–Ag(2)–N(12)	68.2(4)	N(10)–Ag(4)–N(17)	66.2(4)
N(6)–Ag(2)–N(12 <sup>xviii</sup> )	113.7(3)	N(10)–Ag(4)–N(31)	89.0(4)
N(12)–Ag(2)–N(12 <sup>xviii</sup> )	176.8(4)	N(10)–Ag(4)–N(38)	133.6(4)
N(27)–Ag(3)–N(27 <sup>xviii</sup> )	115.0(5)	N(17)–Ag(4)–N(31)	130.3(4)
N(27)–Ag(3)–N(33)	69.3(4)	N(17)–Ag(4)–N(38)	157.1(4)
N(27)–Ag(3)–N(33 <sup>xviii</sup> )	113.0(3)	N(31)–Ag(4)–N(38)	68.4(4)
N(27)–Ag(3)–F(51A/B/C)	153.6(6)/166.5(5)/143.1(5)		
Ag(1)...Ag(2)	3.7443(16)	Ag(2)...Ag(3)	7.4758(16)
Ag(1)...Ag(3)	3.7315(16)	Ag(2)...Ag(4)	6.9279(11)
Ag(1)...Ag(4)	5.8354(9)	Ag(3)...Ag(4)	6.9319(11)

**Table S7.** Metric parameters for intramolecular and intermolecular  $\pi \dots \pi$  interactions in **4·2MeNO<sub>2</sub>** ( $\text{\AA}$ ,  $^\circ$ ). See Fig. S12 for the atom numbering scheme employed. Symmetry code: (vi)  $1-x, y, \frac{3}{2}-z$ ; (vii)  $1-x, -1+y, \frac{3}{2}-z$ ; (viii)  $\frac{1}{2}-x, \frac{1}{2}-y, 1-z$ .

	Dihedral angle	Interplanar distance	Horizontal offset
<b>Intramolecular</b>			
[N(11)–C(15)]...[N(21 <sup>vi</sup> )...C(25 <sup>vi</sup> )]	6.7(7)	3.28(4)	1.82
[N(21)–C(25)]...[C(26)...N(31)]	4.6(6)	3.34(4)	0.84
[N(32)–C(36)]...[N(42 <sup>vi</sup> )...C(46 <sup>vi</sup> )]	5.1(7)	3.23(5)	1.80
[N(42)–C(46)]...[C(5)...N(10)]	5.0(6)	3.35(4)	0.80
<b>Intermolecular</b>			
[N(11)–C(15)]...[N(32 <sup>vii</sup> )–C(36 <sup>vii</sup> )]	9.2(8)	3.37(4)	1.23
[N(16)–C(21)]...[N(16 <sup>viii</sup> )–C(21 <sup>viii</sup> )]	0	3.37(12)	1.13

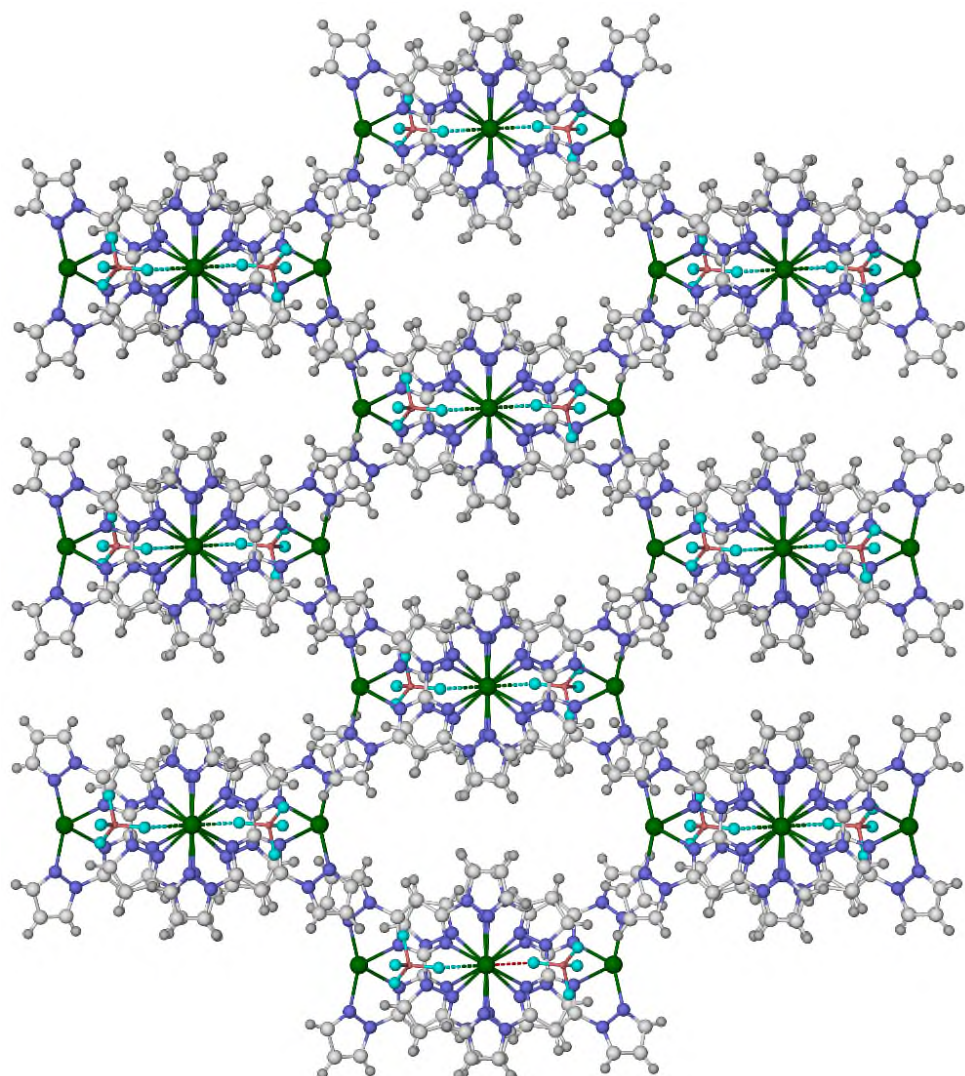


**Figure S13.** Packing diagram of **4·2MeNO<sub>2</sub>**, showing the anion- and solvent-filled voids in the lattice. The view shows the (010) crystal plane, with the *c* axis vertical. All atoms have arbitrary radii.

Colour code: C, white; H, pale grey; Ag, green; B, pink; F, cyan; N, blue.

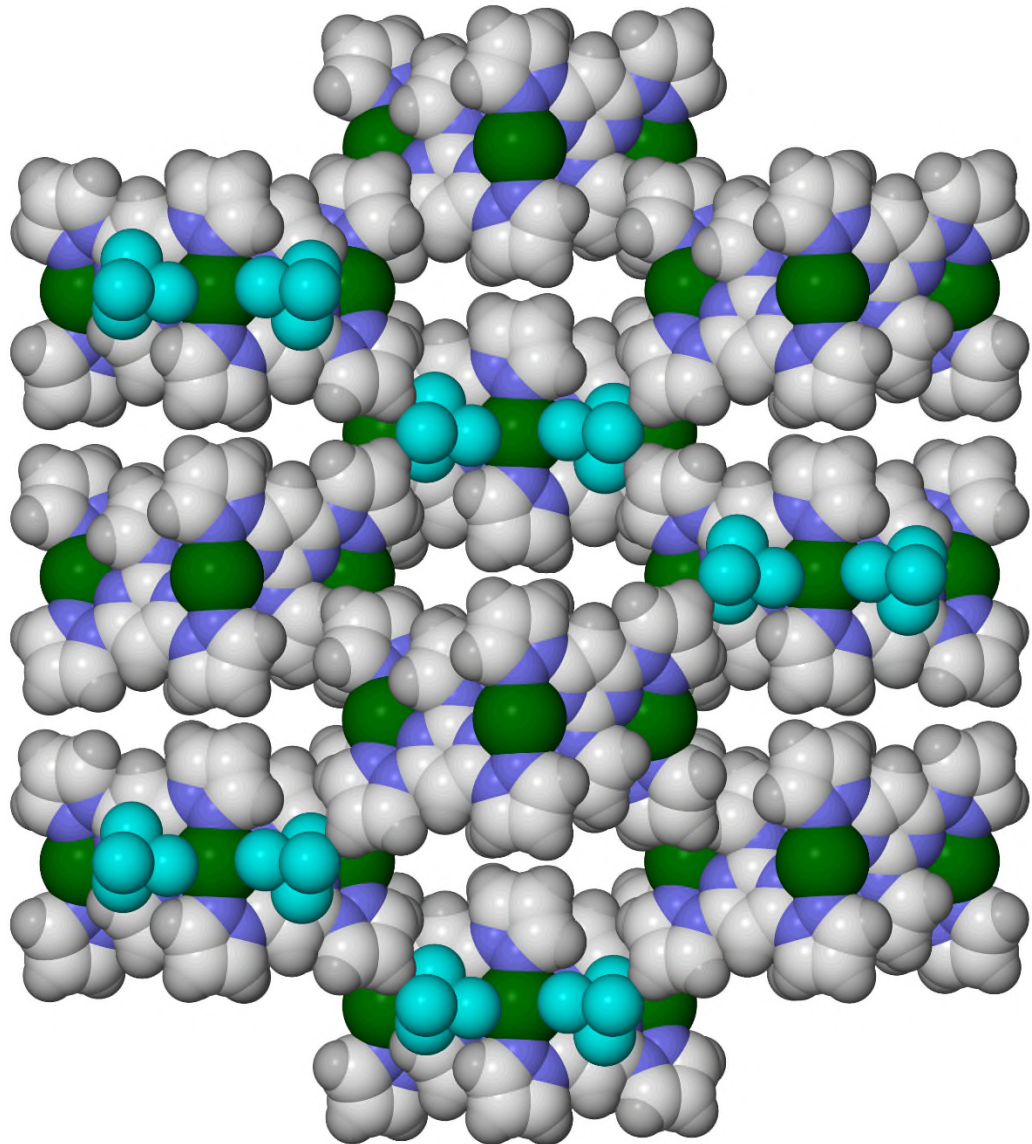


**Figure S14.** Space-filling packing diagram of 4·2MeNO<sub>2</sub>, showing the anion- and solvent-filled voids in the lattice. The view is the same as in Figure S13.

Colour code: C, white; H, pale grey; Ag, green; B, pink; F, cyan; N, blue.

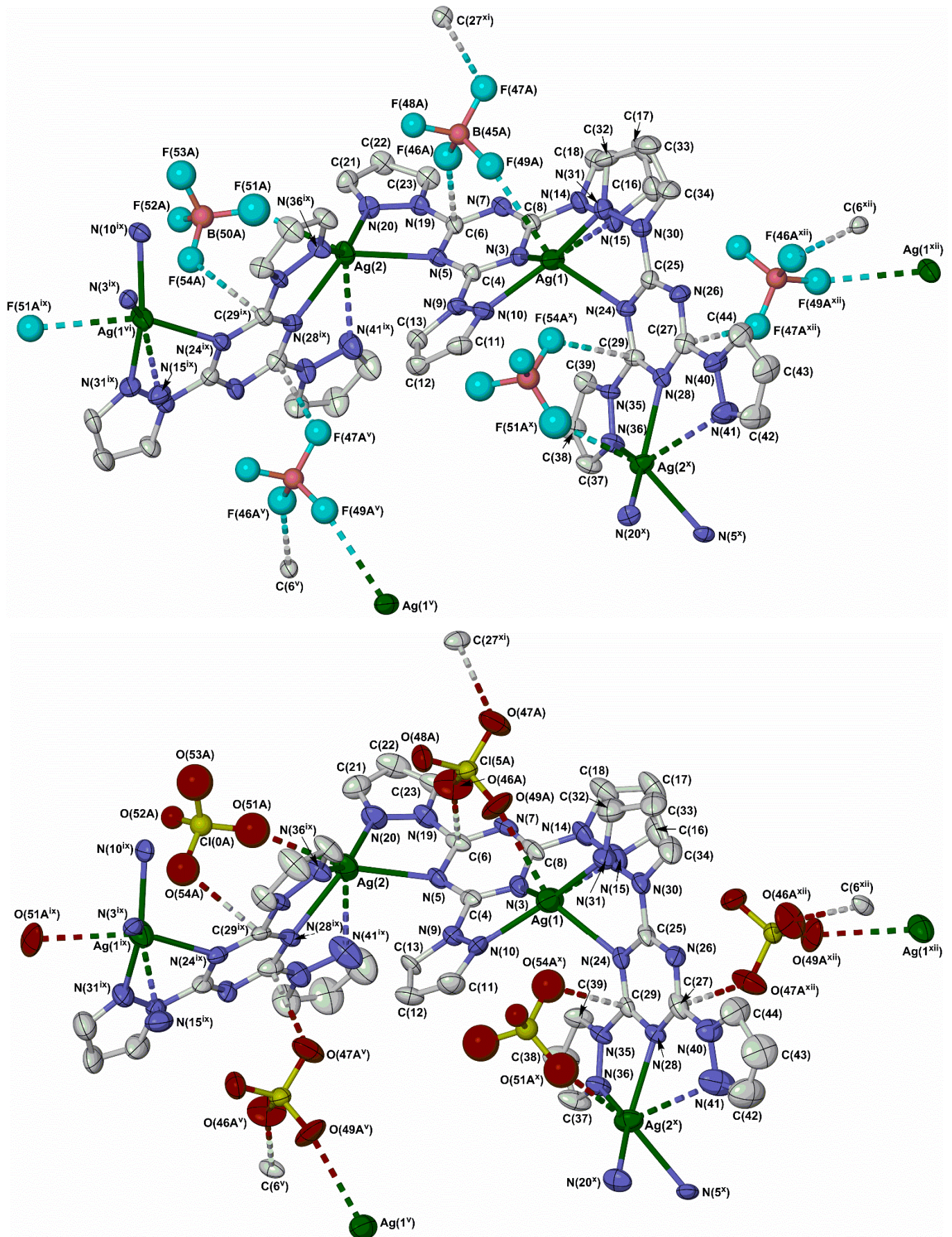


**Figure S15.** Views of the full asymmetric unit of isostructural **[Ag(tpt)]BF<sub>4</sub>** (**5a**, top) and **[Ag(tpt)]ClO<sub>4</sub>** (**5b**, bottom), showing the full atom numbering scheme. Only one orientation of the disordered anions is shown; other details as for Figure S4. Symmetry codes: (v)  $x, -1+y, z$ ; (ix)  $1-x, -y, \frac{1}{2}+z$ ; (x)  $1-x, -y, -\frac{1}{2}+z$ ; (xi)  $1-x, 1-y, \frac{1}{2}+z$ ; (xii)  $1-x, 1-y, -\frac{1}{2}+z$ . Colour code: C, white; Ag, green; B, pink; Cl, yellow; F, cyan; N, blue; O, red.

**Table S8.** Selected bond lengths ( $\text{\AA}$ ) and angles ( $^\circ$ ) for the isostructural complexes **5a** and **5b**, including intramolecular Ag...Ag distances and anion... $\pi$  contacts. See Fig. S15 for the atom numbering schemes employed. Symmetry codes: (ix)  $1-x, -y, \frac{1}{2}+z$ ; (x)  $1-x, -y, -\frac{1}{2}+z$ ; (xii)  $1-x, 1-y, -\frac{1}{2}+z$ .

<b>5a</b>	<b>5b</b>
Ag(1)–N(3)	2.398(6)
Ag(1)–N(10)	2.286(6)
Ag(1)–N(15)	2.951(7)
Ag(1)–N(24)	2.573(6)
Ag(1)–N(31)	2.193(6)
Ag(1)–F(49A/B)	2.971(9)/3.133(16)
Ag(2)–N(5)	2.466(6)
Ag(2)–N(20)	2.245(5)
Ag(2)–N(28 <sup>ix</sup> )	2.400(6)
Ag(2)–N(36 <sup>ix</sup> )	2.286(6)
Ag(2)–N(41 <sup>ix</sup> )	2.906(8)
Ag(2)–F(51A/B)	2.795(15)/2.904(13)
N(3)–Ag(1)–N(10)	70.0(2)
N(3)–Ag(1)–N(15)	58.84(19)
N(3)–Ag(1)–N(24)	132.64(19)
N(3)–Ag(1)–N(31)	131.8(2)
N(3)–Ag(1)–F(49A/B)	79.1(2)/84.5(3)
N(10)–Ag(1)–N(15)	126.2(2)
N(10)–Ag(1)–N(24)	109.8(2)
N(10)–Ag(1)–N(31)	153.5(3)
N(10)–Ag(1)–F(49A/B)	93.4(2)/99.3(4)
N(15)–Ag(1)–N(24)	94.13(19)
N(15)–Ag(1)–N(31)	79.8(2)
N(15)–Ag(1)–F(49A/B)	92.4(2)/91.7(3)
N(24)–Ag(1)–N(31)	68.5(2)
N(24)–Ag(1)–F(49A/B)	145.2(2)/138.5(3)
N(31)–Ag(1)–F(49A/B)	79.1(2)/72.2(4)
N(5)–Ag(2)–N(20)	69.8(2)
N(5)–Ag(2)–N(28 <sup>ix</sup> )	124.35(19)
N(5)–Ag(2)–N(36 <sup>ix</sup> )	113.7(2)
N(5)–Ag(2)–N(41 <sup>ix</sup> )	81.5(2)
N(5)–Ag(2)–F(51A/B)	147.3(4)/140.7(3)
N(20)–Ag(2)–N(28 <sup>ix</sup> )	141.1(2)
N(20)–Ag(2)–N(36 <sup>ix</sup> )	144.0(2)
N(20)–Ag(2)–N(41 <sup>ix</sup> )	91.8(2)
N(20)–Ag(2)–F(51A/B)	77.7(4)/72.9(3)
N(28 <sup>ix</sup> )–Ag(2)–N(36 <sup>ix</sup> )	68.9(2)
N(28 <sup>ix</sup> )–Ag(2)–N(41 <sup>ix</sup> )	59.6(2)
N(28 <sup>ix</sup> )–Ag(2)–F(51A/B)	84.0(4)/92.8(3)
N(36 <sup>ix</sup> )–Ag(2)–N(41 <sup>ix</sup> )	124.1(2)
N(36 <sup>ix</sup> )–Ag(2)–F(51A/B)	90.4(4)/89.8(3)
N(41 <sup>ix</sup> )–Ag(2)–F(51A/B)	103.8(4)/111.9(3)
Ag(1)...Ag(2)	6.2119(9)
Ag(1)...Ag(2 <sup>x</sup> )	6.5299(8)
C(6)...F(46A/B)	2.869(11)/2.955(17)
C(27)...F(47A <sup>xii</sup> )/F(48B <sup>xii</sup> )	2.892(19)/2.968(12)
C(29)...F(54A/B <sup>x</sup> )	2.998(14)/2.860(14)
Ag(1)–N(3)	2.395(10)
Ag(1)–N(10)	2.285(10)
Ag(1)–N(15)	2.964(12)
Ag(1)–N(24)	2.586(9)
Ag(1)–N(31)	2.210(10)
Ag(1)–O(49A/B)	2.897(15)/2.95(5)
Ag(2)–N(5)	2.469(9)
Ag(2)–N(20)	2.218(9)
Ag(2)–N(28 <sup>ix</sup> )	2.423(8)
Ag(2)–N(36 <sup>ix</sup> )	2.300(9)
Ag(2)–N(41 <sup>ix</sup> )	2.950(13)
Ag(2)–O(51A/B/C)	2.91(3)/2.892(19)/2.70(2)
N(3)–Ag(1)–N(10)	70.2(3)
N(3)–Ag(1)–N(15)	58.9(3)
N(3)–Ag(1)–N(24)	130.4(3)
N(3)–Ag(1)–N(31)	131.9(4)
N(3)–Ag(1)–O(49A/B)	81.6(4)/81.5(10)
N(10)–Ag(1)–N(15)	126.1(3)
N(10)–Ag(1)–N(24)	109.5(3)
N(10)–Ag(1)–N(31)	154.0(4)
N(10)–Ag(1)–O(49A/B)	94.9(6)/97.6(13)
N(15)–Ag(1)–N(24)	91.7(3)
N(15)–Ag(1)–N(31)	79.7(4)
N(15)–Ag(1)–O(49A/B)	94.4(5)/91.8(12)
N(24)–Ag(1)–N(31)	68.5(3)
N(24)–Ag(1)–O(49A/B)	144.4(5)/143.2(11)
N(31)–Ag(1)–O(49A/B)	78.1(5)/76.2(12)
N(5)–Ag(2)–N(20)	70.2(4)
N(5)–Ag(2)–N(28 <sup>vi</sup> )	121.4(3)
N(5)–Ag(2)–N(36 <sup>vi</sup> )	113.0(3)
N(5)–Ag(2)–N(41 <sup>vi</sup> )	80.9(4)
N(5)–Ag(2)–O(51A/B/C)	147.3(6)/141.0(4)/145.9(6)
N(20)–Ag(2)–N(28 <sup>vi</sup> )	140.7(3)
N(20)–Ag(2)–N(36 <sup>vi</sup> )	145.7(4)
N(20)–Ag(2)–N(41 <sup>vi</sup> )	90.0(4)
N(20)–Ag(2)–O(51A/B/C)	78.5(7)/80.8(4)/76.8(6)
N(28 <sup>vi</sup> )–Ag(2)–N(36 <sup>vi</sup> )	69.0(3)
N(28 <sup>vi</sup> )–Ag(2)–N(41 <sup>vi</sup> )	58.9(3)
N(28 <sup>vi</sup> )–Ag(2)–O(51A/B/C)	78.3(7)/68.3(4)/89.6(6)
N(36 <sup>vi</sup> )–Ag(2)–N(41 <sup>vi</sup> )	124.2(3)
N(36 <sup>vi</sup> )–Ag(2)–O(51A/B/C)	98.0(7)/105.7(4)/89.8(7)
N(41 <sup>vi</sup> )–Ag(2)–O(51A/B/C)	90.3(8)/73.4(4)/107.7(7)
Ag(1)...Ag(2)	6.2276(15)
Ag(1)...Ag(2 <sup>x</sup> )	6.5019(14)
C(6)...O(46A/B)	2.889(14)/3.01(4)
C(27)...O(47A/B <sup>xii</sup> )	3.01(2)/2.99(5)
C(29)...O(54A/B/C <sup>x</sup> )	3.10(3)/3.07(3)/2.97(3)

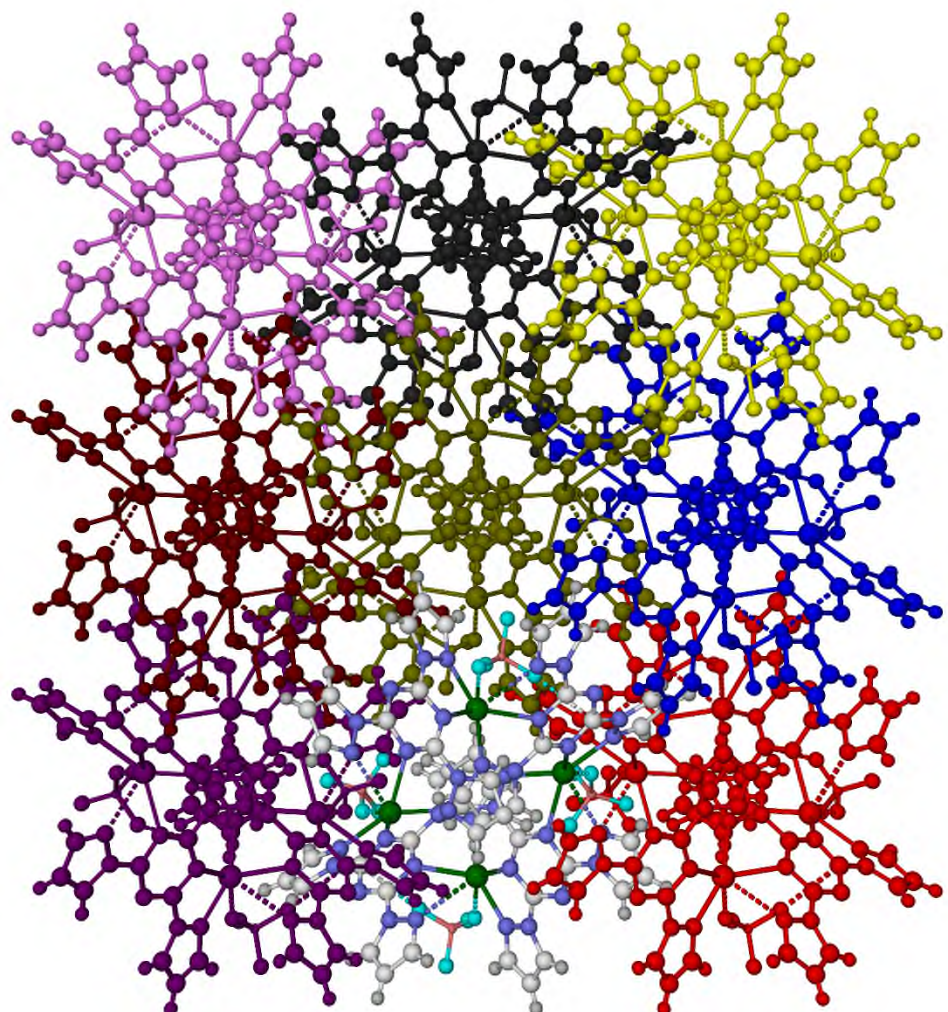
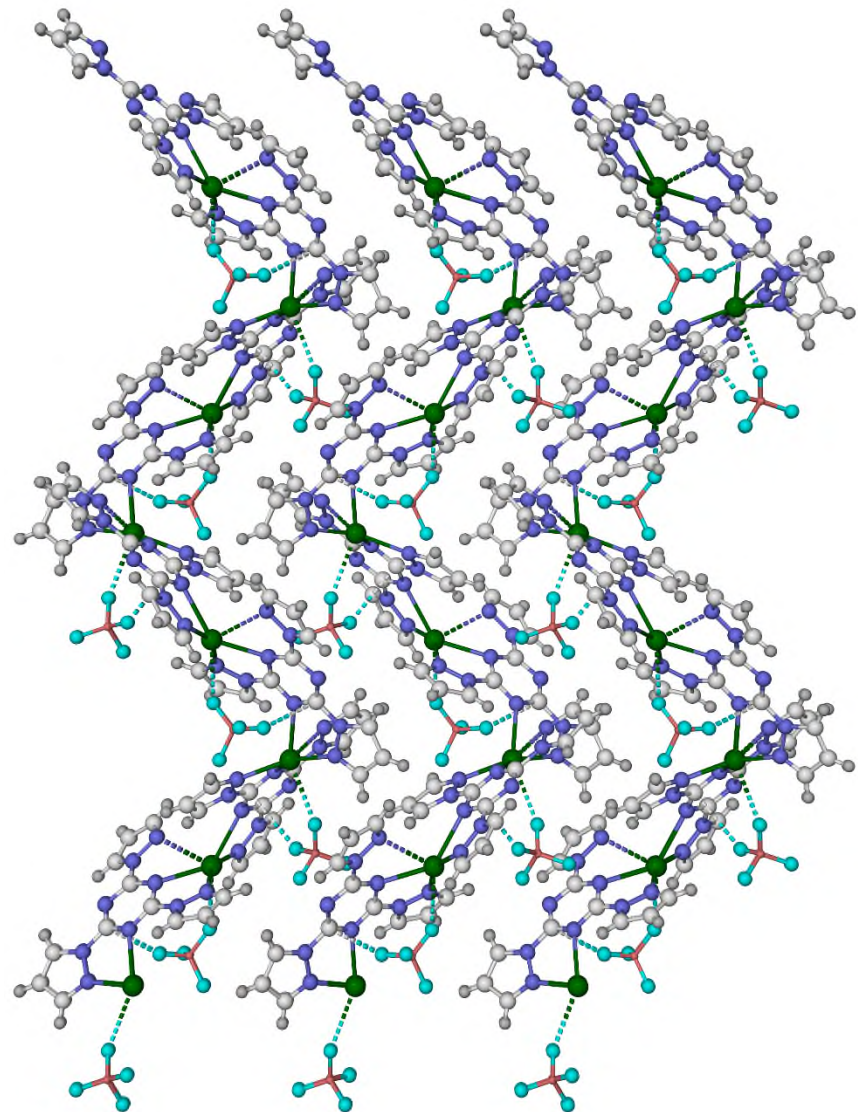


**Figure S16.** Packing diagrams of **5a**, showing the coparallel helical chains in the lattice. Only one orientation of the disordered anions is shown, and all atoms have arbitrary radii. Left: view shows the (010) crystal plane, with the *c* axis vertical. Colour code: C, white; H, pale grey; Ag, green; B, pink; F, cyan; N, blue. Right: view shows the (001) crystal plane with the *b* axis vertical. Each polymer chain is plotted with a different colour scheme, for clarity.

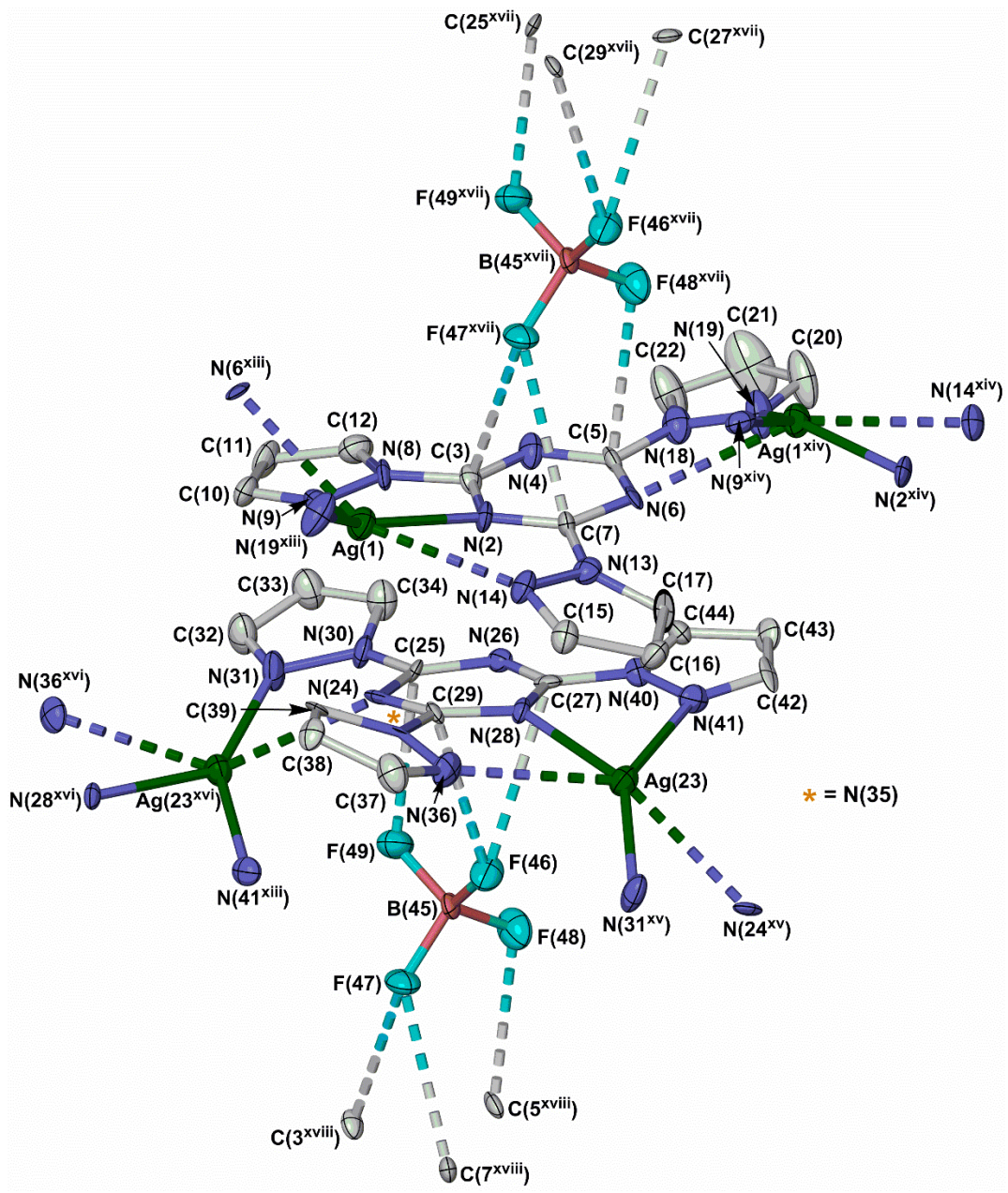


**Figure S17.** Views of the  $\{\text{Ag}(\text{tpt})\}_2(\text{BF}_4)^+$  coordination polymer asymmetric unit of **5a**· $\text{MeNO}_2$ , showing the full atom numbering schemes. The other  $\text{BF}_4^-$  ion and solvent, which do not take part in anion... $\pi$  interactions, are omitted for clarity. Other details as for Figure S4.

Symmetry codes: (xiii)  $2-x, \frac{1}{2}+y, 1-z$ ; (xiv)  $2-x, -\frac{1}{2}+y, 1-z$ ; (xv)  $1-x, -\frac{1}{2}+y, 1-z$ ; (xvi)  $1-x, \frac{1}{2}+y, 1-z$ ; (xvii)  $1+x, y, z$ ; (xviii)  $-1+x, y, z$ . Colour code: C, white; H, pale grey; Ag, green; B, pink; F, cyan; N, blue; O, red.

**Table S9.** Selected bond lengths ( $\text{\AA}$ ) and angles ( $^\circ$ ) for **5a**·MeNO<sub>2</sub>, including intramolecular Ag...Ag distances and anion... $\pi$  contacts. See Fig. S17 for the atom numbering scheme employed. Symmetry codes: (xiii) 2-x,  $1/2+y$ , 1-z; (xiv) 2-x,  $-1/2+y$ , 1-z; (xv) 1-x,  $-1/2+y$ , 1-z; (xvi) 1-x,  $1/2+y$ , 1-z; (xvii) 1+x, y, z.

Ag(1)-N(2)	2.388(11)	Ag(23)-N(24 <sup>xv</sup> )	2.821(10)
Ag(1)-N(6 <sup>xiii</sup> )	2.849(10)	Ag(23)-N(28)	2.376(10)
Ag(1)-N(9)	2.372(11)	Ag(23)-N(31 <sup>xv</sup> )	2.223(12)
Ag(1)-N(14)	2.832(11)	Ag(23)-N(36)	2.877(12)
Ag(1)-N(19 <sup>xiii</sup> )	2.226(12)	Ag(23)-N(41)	2.416(11)
N(2)-Ag(1)-N(6 <sup>xiii</sup> )	128.8(3)	N(24 <sup>xv</sup> )-Ag(23)-N(28)	127.9(3)
N(2)-Ag(1)-N(9)	68.8(4)	N(24 <sup>xv</sup> )-Ag(23)-N(31 <sup>xv</sup> )	64.8(4)
N(2)-Ag(1)-N(14)	61.9(4)	N(24 <sup>xv</sup> )-Ag(23)-N(36)	139.3(3)
N(2)-Ag(1)-N(19 <sup>xiii</sup> )	144.6(5)	N(24 <sup>xv</sup> )-Ag(23)-N(41)	83.1(3)
N(6 <sup>xiii</sup> )-Ag(1)-N(9)	85.1(3)	N(28)-Ag(23)-N(31 <sup>xv</sup> )	140.4(4)
N(6 <sup>xiii</sup> )-Ag(1)-N(14)	139.2(3)	N(28)-Ag(23)-N(36)	62.4(3)
N(6 <sup>xiii</sup> )-Ag(1)-N(19 <sup>xiii</sup> )	63.3(4)	N(28)-Ag(23)-N(41)	67.9(4)
N(9)-Ag(1)-N(14)	128.1(4)	N(31 <sup>xv</sup> )-Ag(23)-N(36)	84.7(4)
N(9)-Ag(1)-N(19 <sup>xiii</sup> )	144.0(4)	N(31 <sup>xv</sup> )-Ag(23)-N(41)	146.4(4)
N(14)-Ag(1)-N(19 <sup>xiii</sup> )	87.8(4)	N(36)-Ag(23)-N(41)	128.5(4)
Ag(1)...Ag(1 <sup>xiv</sup> )	6.9609(9)	Ag(23)...Ag(23 <sup>xvi</sup> )	6.9518(8)
$\tau[\text{Ag}(1)]^a$	0.09	$\tau[\text{Ag}(23)]^a$	0.02
C(3)...F(47 <sup>xvii</sup> )	3.016(13)	C(25)...F(49)	2.897(15)
C(5)...F(48 <sup>xvii</sup> )	2.929(15)	C(27)...F(46)	3.092(14)
C(7)...F(47 <sup>xvii</sup> )	2.995(15)	C(29)...F(46)	2.980(14)

<sup>a</sup>See ref. [1] for the definition of  $\tau$  (page 4). An ideal square pyramidal geometry gives  $\tau = 0$ , while an ideal trigonal bipyramidal geometry yields  $\tau = 1$ .

**Table S10.** Metric parameters for intra-chain and inter-chain  $\pi\ldots\pi$  interactions in **5a**·MeNO<sub>2</sub> ( $\text{\AA}$ ,  $^\circ$ ). See Fig. S17 for the atom numbering scheme employed. Symmetry code: (xiii) 2-x,  $1/2+y$ , 1-z; (xvi) 1-x,  $1/2+y$ , 1-z.

	Dihedral angle	Interplanar distance	Horizontal offset
<b>Intra-chain</b>			
[N(8)-C(12)]...[N(13 <sup>xiii</sup> )...C(17 <sup>xiii</sup> )]	11.2(4)	3.27(4)	1.02
[N(35)-C(39)]...[N(40 <sup>xvi</sup> )...C(44 <sup>xvi</sup> )]	11.91(4)	3.38(3)	0.71
<b>Inter-chain</b>			
[N(2)-C(12)]...[N(24)...C(34)]	2.5(2)	3.25(5)	1.32

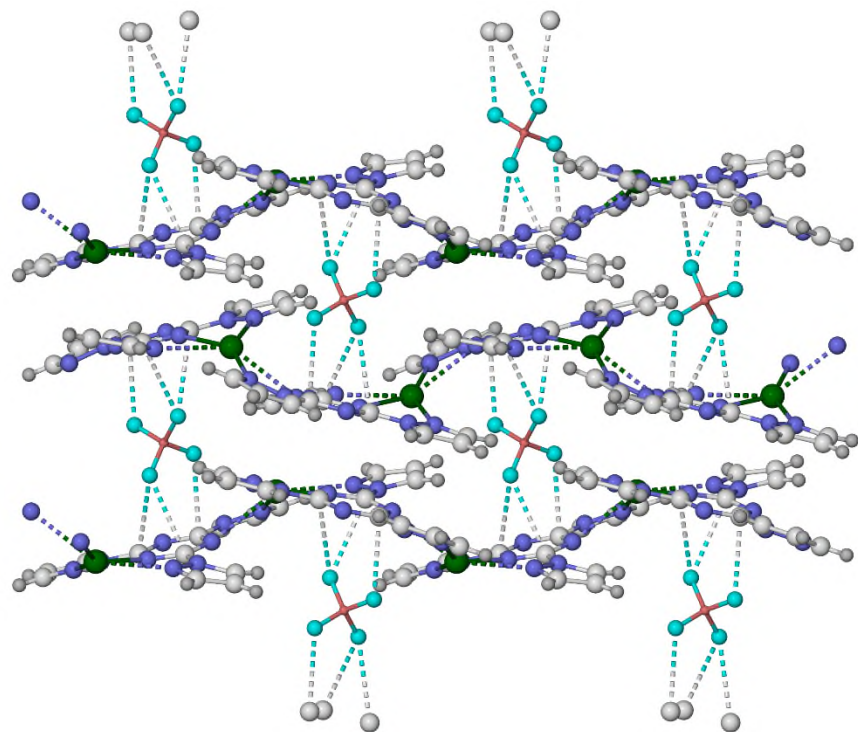


**Figure S18.** Packing diagram of **5a**·MeNO<sub>2</sub>, showing the anion... $\pi$  interactions linking the zig-zag coordination polymer chains. The view is parallel to the [105] crystal vector, with the *b* axis horizontal. All atoms have arbitrary radii. Colour code: C, white; H, pale grey; Ag, green; B, pink; F, cyan; N, blue.

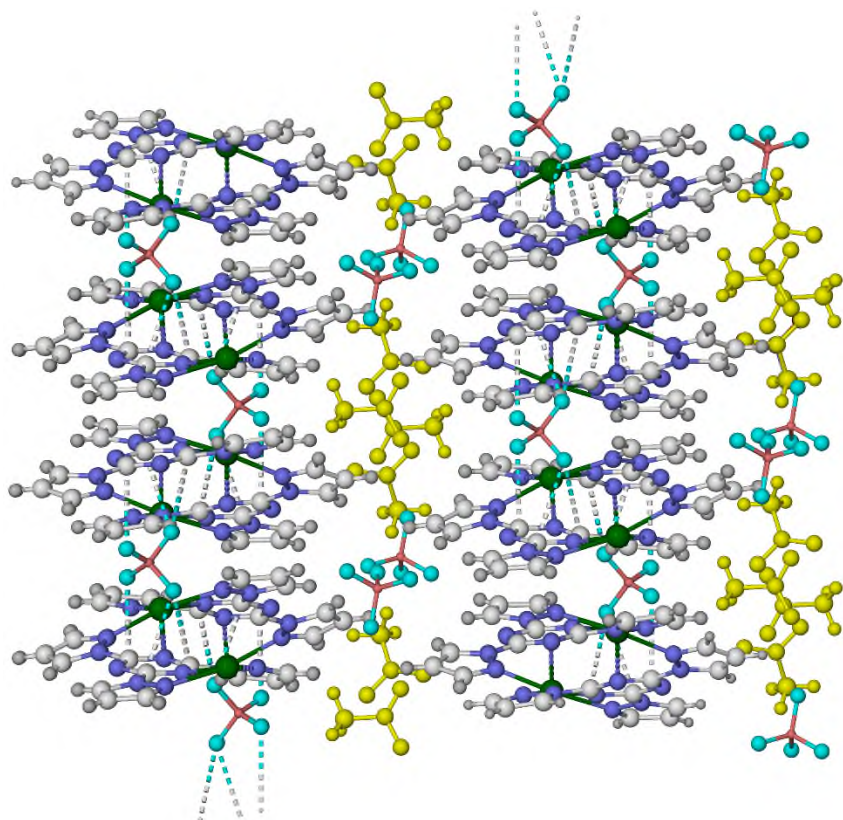


**Figure S19.** Packing diagram of **5a**·MeNO<sub>2</sub>, showing the coordination polymer/anion... $\pi$  layers separated by the remaining anions and solvent. The view shows the (010) crystal plane, with the *a* axis vertical. All atoms have arbitrary radii. Colour code: C, white; H, pale grey; Ag, green; B, pink; F, cyan; N, blue; MeNO<sub>2</sub>, yellow.

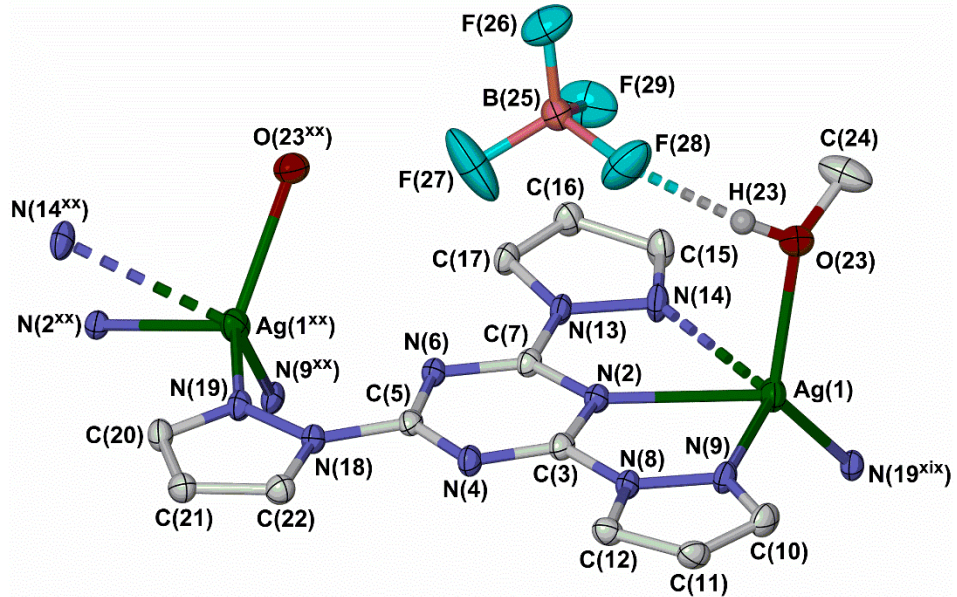


**Figure S20.** View of the full  $[\text{Ag}(\text{tpt})(\text{MeOH})]\text{BF}_4$  asymmetric unit of **5a**·MeOH, showing the full atom numbering schemes. Details as for Figure S4. Symmetry codes: (xix)  $\frac{1}{2}+x, y, \frac{3}{2}-z$ ; (xx)  $-\frac{1}{2}+x, y, \frac{3}{2}-z$ . Colour code: C, white; H, pale grey; Ag, green; B, pink; F, cyan; N, blue; O, red.

**Table S11.** Selected bond lengths ( $\text{\AA}$ ) and angles ( $^\circ$ ) for **5a**·MeOH, including intramolecular Ag...Ag distances.

See Fig. S20 for the atom numbering schemes employed. Symmetry codes: (xix)  $\frac{1}{2}+x, y, \frac{3}{2}-z$ ; (xx)  $-\frac{1}{2}+x, y, \frac{3}{2}-z$ .

Ag(1)–N(2)	2.458(2)	Ag(1)–N(19 <sup>xix</sup> )	2.217(2)
Ag(1)–N(9)	2.381(2)	Ag(1)–O(23)	2.387(2)
Ag(1)–N(14)	2.797(2)		
N(2)–Ag(1)–N(9)	68.10(7)	N(9)–Ag(1)–N(19 <sup>xix</sup> )	122.93(8)
N(2)–Ag(1)–N(14)	60.61(7)	N(9)–Ag(1)–O(23)	96.60(7)
N(2)–Ag(1)–N(19 <sup>xix</sup> )	124.21(7)	N(14)–Ag(1)–N(19 <sup>xix</sup> )	88.93(7)
N(2)–Ag(1)–O(23)	96.43(7)	N(14)–Ag(1)–O(23)	87.78(7)
N(9)–Ag(1)–N(14)	128.68(7)	N(19 <sup>xix</sup> )–Ag(1)–O(23)	130.25(7)
Ag(1)...Ag(1 <sup>xx</sup> )	7.7359(2)	$\tau^a$	0.03

<sup>a</sup>See ref. [1] for the definition of  $\tau$  (page 4). An ideal square pyramidal geometry gives  $\tau = 0$ , while an ideal trigonal bipyramidal geometry yields  $\tau = 1$ .

**Table S12.** Hydrogen bond parameters ( $\text{\AA}$ ,  $^\circ$ ) for **5a**·MeOH. See Fig. S20 for the atom numbering scheme.

	O–H	H...F	O...F	O–H...F
O(23)–H(23)...F(28)	0.80(4)	1.94(4)	2.727(3)	166(4)

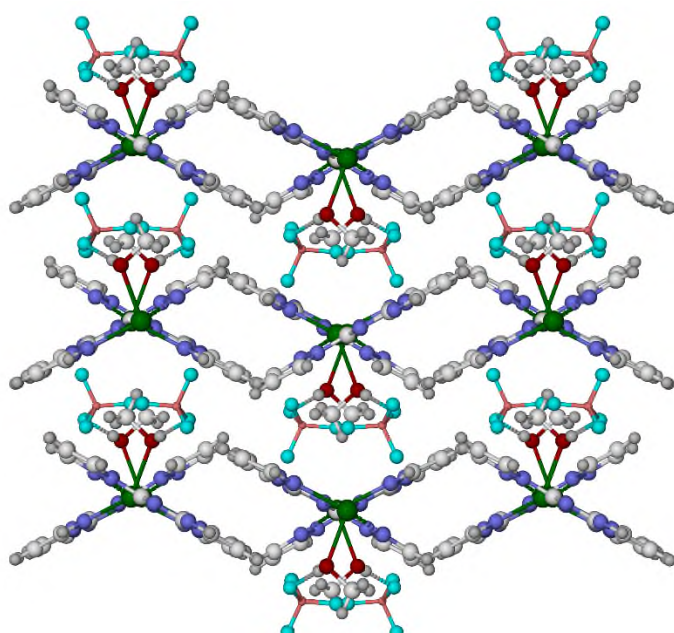


**Figure S21.** Packing diagram of **5a**·MeOH, showing well-separated polymer chains in the lattice. The view shows the (100) crystal plane, with the unit cell *c* axis horizontal. Colour code: C, white; H, pale grey; Ag, green; B, pink; F, cyan; N, blue; O, red.

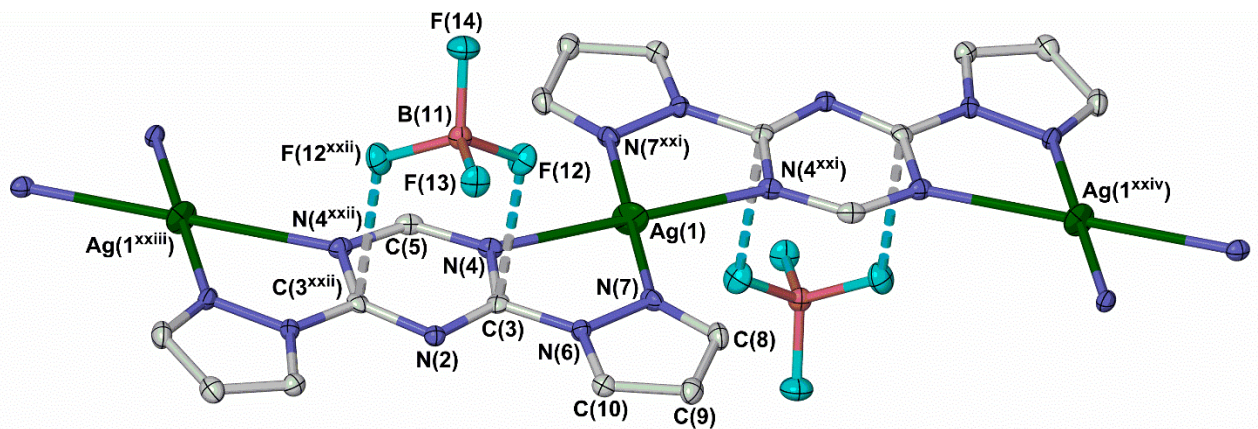


**Figure S22.** View of the  $\{[\text{Ag}(\text{bpt})]\text{BF}_4\}_n$  coordination polymer chain in **6**, showing the full atom numbering scheme. Details as for Figure S4. Symmetry codes: (xxi)  $2-x, 1-y, -z$ ; (xxii)  $x, \frac{3}{2}-y, z$ ; (xxiii)  $2-x, \frac{1}{2}+y, -z$ ; (xxiv)  $2-x, -\frac{1}{2}+y, -z$ . Colour code: C, white; Ag, green; B, pink; F, cyan; N, blue.

**Table S13.** Selected bond lengths ( $\text{\AA}$ ) and angles ( $^\circ$ ) for **6**, including intramolecular Ag...Ag distances and anion.... $\pi$  contacts. See Fig. S22 for the atom numbering scheme employed. Symmetry codes: (xxi)  $2-x, 1-y, -z$ ; (xxiii)  $2-x, \frac{1}{2}+y, -z$ .

Ag(1)–N(4)	2.523(2)
Ag(1)–N(7)	2.289(4)
N(4)–Ag(1)–N(4 <sup>xxi</sup> )	180
N(4)–Ag(1)–N(7)	68.71(7)
N(4)–Ag(1)–N(7 <sup>xxi</sup> )	111.29(7)
N(7)–Ag(1)–N(7 <sup>xxi</sup> )	180
Ag(1)...Ag(1 <sup>xxiii</sup> )	7.1038(2)
C(3)...F(12)	2.823(3)

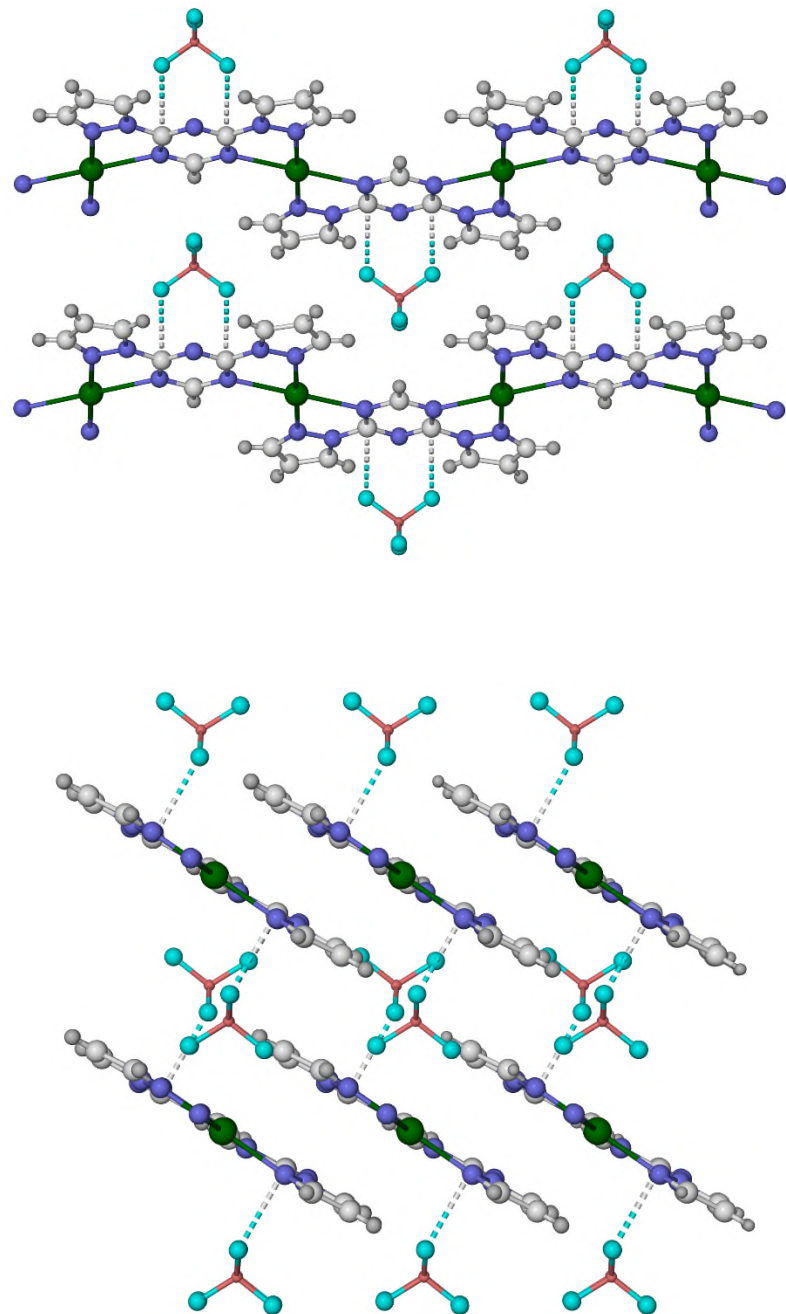


**Figure S23.** Two packing diagrams of **6**, showing the planar coordination polymer chains and anion... $\pi$  interactions. Top: view parallel to the [100] crystal vector, with the *b* axis horizontal. Bottom: view shows the (010) crystal plane with the *c* axis horizontal. All atoms have arbitrary radii. Colour code: C, white; H, pale grey; Ag, green; B, pink; F, cyan; N, blue.

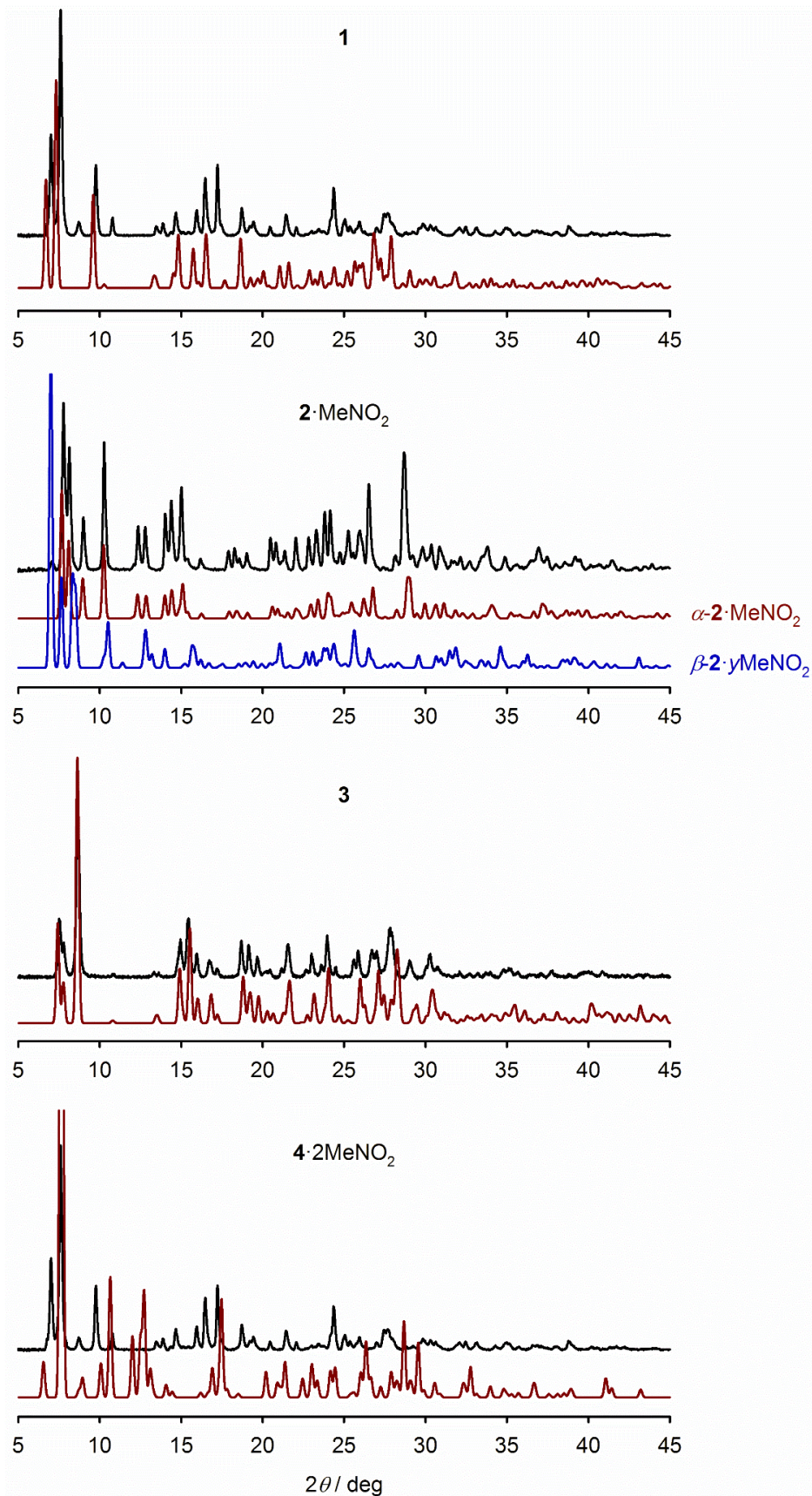


**Figure S24.** Measured (black) and simulated (red, blue) powder diffraction data from the tpp and tpym complexes.

Bulk samples of **2·MeNO<sub>2</sub>**, which retains its lattice solvent, predominantly contain the  $\alpha$ -form of the compound. Discrepancies between the measured and simulated data for **1** and **4** may reflect desolvation of the samples (their crystals contain lattice solvent, but the dried materials are solvent-free by microanalysis).

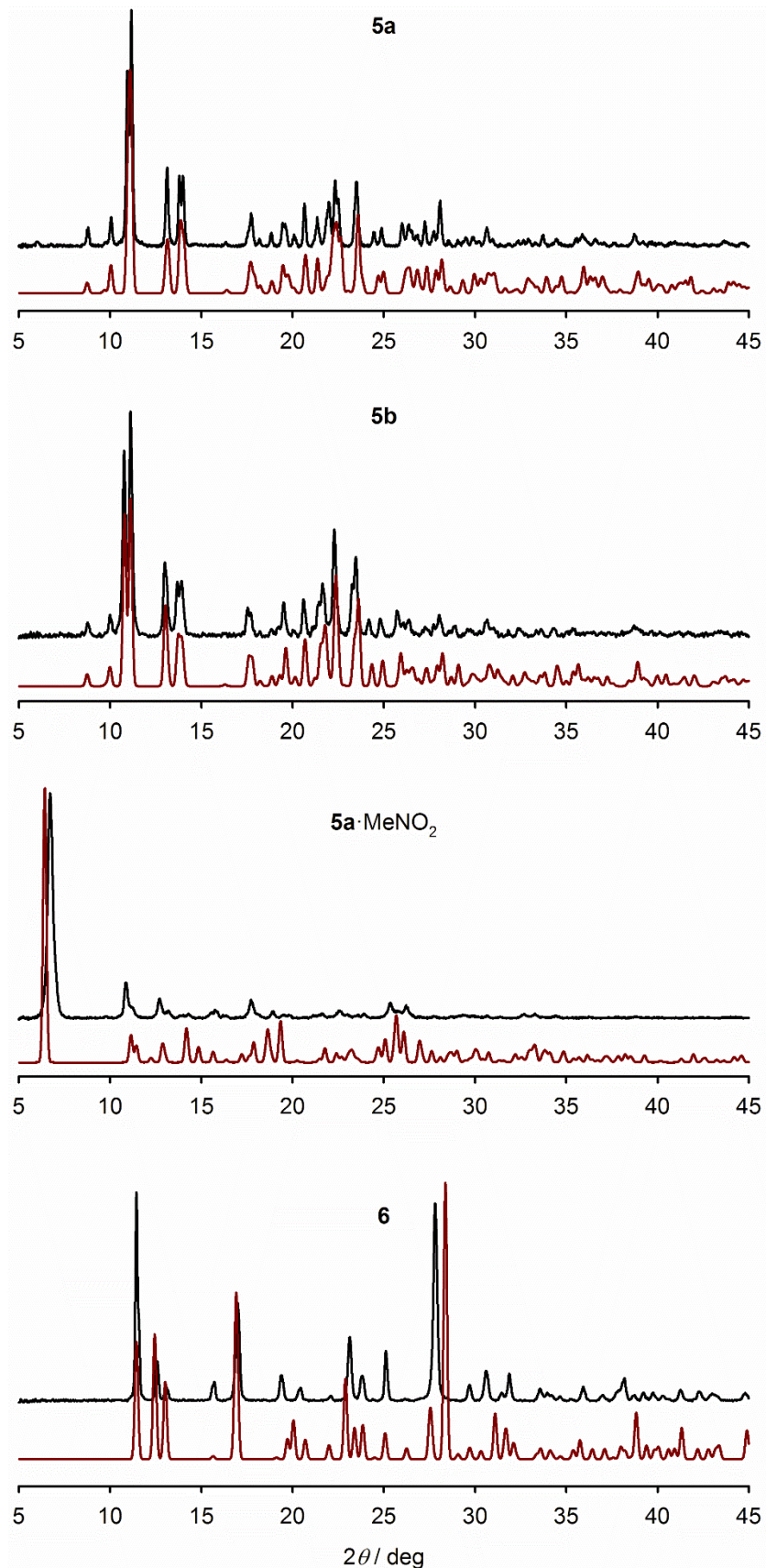
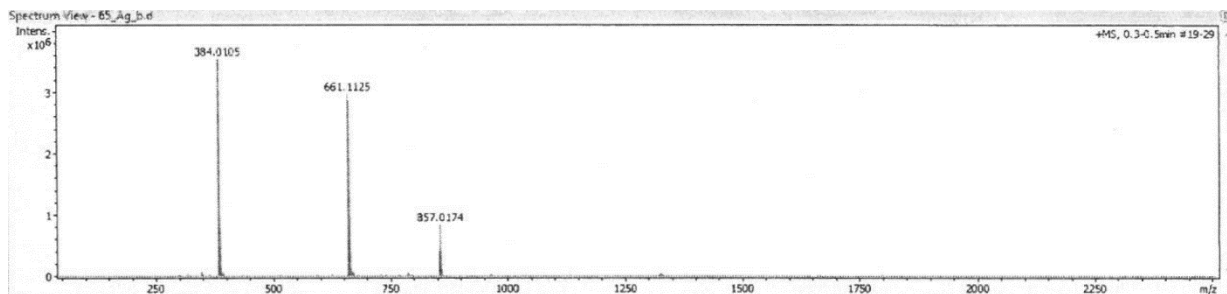
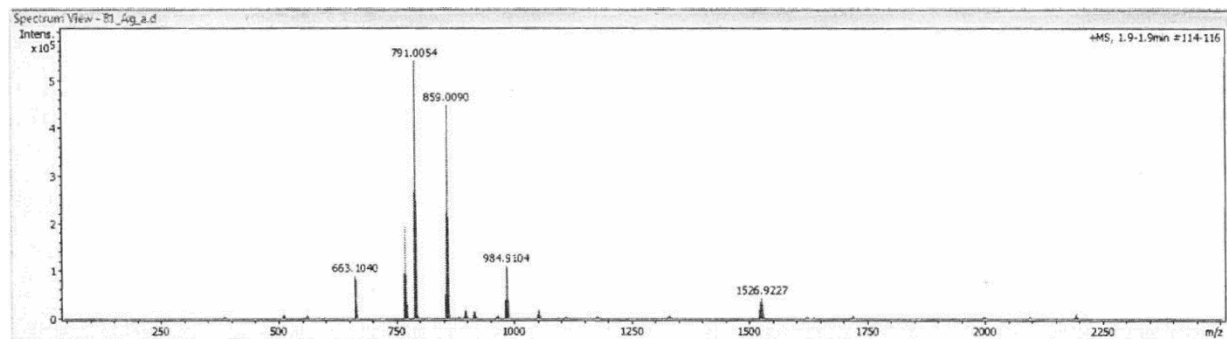


**Figure S25.** Measured (black) and simulated (red) powder diffraction data from the tpt and bpt complexes.

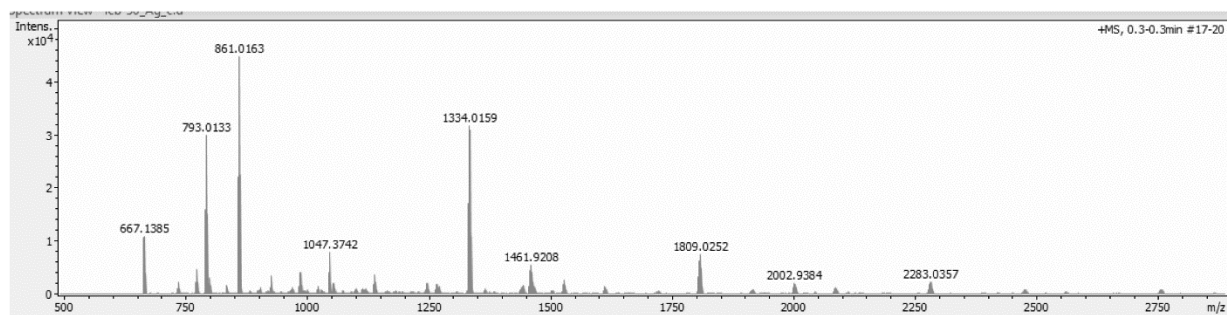
2



4



5



6

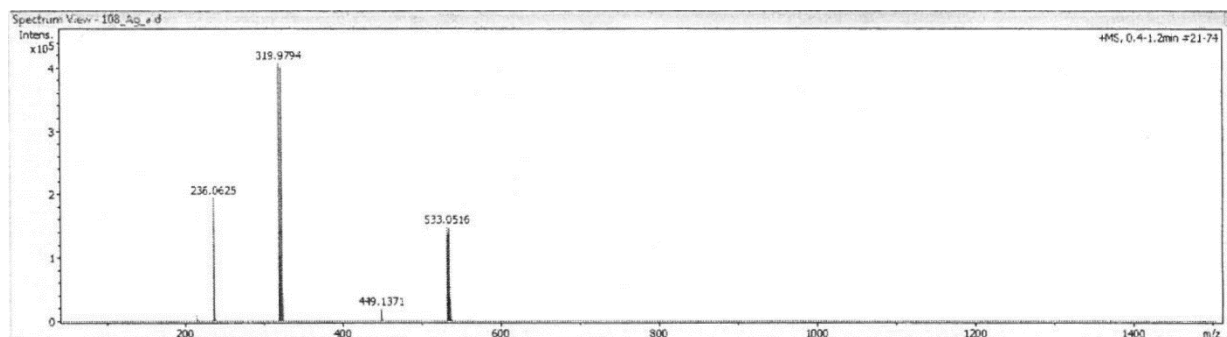


**Figure S26.** Electrospray mass spectra of the silver complexes of tpp, tpym, tpt and bpt from MeNO<sub>2</sub> solution.

Peak assignments are listed in the Experimental Section of the main article.